BALLISTIC RESEARCH LABORATORIES

REPORT NO. 1183

DECEMBER 1962

THE SIMULATION OF INTERIOR BALLISTIC PERFORMANCE OF GUNS BY DIGITAL COMPUTER PROGRAM

Paul G. Baer

Jerome M. Frankle

Interior Ballistics Laboratory

RDT & E Project No. 1M010501A004

ABERDEEN PROVING GROUND, MARYLAND

ERRATA-BRLR 1183

pg 8 m_i specific mass of i th propellant, lb-mol/lb

pg 9 R Universal Gas Constant, in-lb/lb-mol-°K

T_s initial temperature of gun, °K

pg 14 $\bar{c}_{p_i} - \bar{c}_{v_i} = m_i R$

pg 15 dx (in Eq(14))

pg 16 and pg 23

$$E_h = \frac{12 \times 0.38 c^{1.5} \left(x_m + \frac{V_o}{A}\right) \left(\frac{\sum_{i=1}^{n} C_i \, To_i}{\sum_{i=1}^{n} C_i} - T_s \right) v^2}{\left[1 + \frac{0.6 c^{2.175}}{\left(\sum_{i=1}^{n} C_i \right)^{0.8375}} \right] v_m^{\,2}}$$

pg 19 and pg 24

$$p_o = \frac{p_b}{(1-a_o)^{n'+1}}$$

pg 46 B16 IF (Y1>0)GOTO(B17)%Y1=0% IF(Y3 etc

J. M. Frankle

B A L L I S T I C R E S E A R C H L A B O R A T O R I E S

REPORT NO. 1183

PGBaer/JMFrankle/mec
Aberdeen Proving Ground, Md.
December 1962

THE SIMULATION OF INTERIOR BALLISTIC PERFORMANCE OF GUNS BY DIGITAL COMPUTER PROGRAM

ABSTRACT

When non-conventional guns are to be considered or when detailed design information is required, interior ballistic calculations become more difficult and time-consuming. To deal with these problems, the equations which describe the interior ballistic performance of guns and gun-like weapons have been programmed for the high-speed digital computers available at the Ballistic Research Laboratories. The major innovation contained in the equations derived in this report is the provision for use of propellant charges made up of several propellants of different chemical compositions and different granulations. Results obtained by the method described in this report compare favorably with those of other interior ballistic systems. In addition, considerably more detail is obtained in far less time. A comparison with experimental data from well-instrumented gun-firings is also presented to demonstrate the validity of this method of computation.

TABLE OF CONTENTS

LIST OF SYMBOLS

a acceleration of projectile, in./sec^2

a_o constant defined by Equation (28a), dimensionless

A area of base of projectile including appropriate portion of rotating band, in.^{2}

b_i covolume of i th propellant, in.^{3}/lb

c diameter of bore, in.

c_{v_i} specific heat at constant volume of i th propellant (c_{v_i} is a function of T), in.-lb/lb-^oK

$\bar{c}_{v_i}$ mean value of specific heat at constant volume of i th propellant (over temperature range T to T_{o_i}), in.-lb/lb-^oK

$\bar{c}_{p_i}$ mean value of specific heat at constant pressure of i th propellant (over temperature range T to T_{o_i}), in.-lb/lb-^oK

C_i initial weight of i th propellant, lb

C_I initial weight of igniter, lb

d_i diameter of perforation in i th propellant grains, in.

dt incremental time, sec

dT incremental temperature, ^oK

dx incremental distance traveled by projectile, in.

$\frac{dz_i}{dt}$ mass fraction burning rate for i th propellant, sec^{-1}

D_i outside diameter of i th propellant grains, in.

E_h energy lost due to heat loss, in.-lb

E_p kinetic energy of propellant gas and unburned propellant, in.-lb

E_{pr} energy lost due to bore friction and engraving of rotating band, in.-lb

f_i functional relationship between S_i and z_i

F_a resultant axial force on projectile, lb

F_f frictional force on projectile, lb

F_i "force" of i th propellant, in.-lb/lb

F_I "force" of igniter propellant, in.-lb/lb

F_p propulsive force on base of projectile, lb

F_r gas retardation force, lb

g constant for conversion of weight units to mass units, $in./sec^2$

G functional relationship between p_r and x

K_v burning rate velocity coefficient, $\frac{in.}{sec}$ in./sec

K_x burning rate displacement coefficient, $\frac{in.}{sec\text{-}in.}$

L_i length of i th propellant grains, in.

m_i specific mass of i th propellant, lb-mols/mol

M mass of projectile, slugs/12

n number of propellants, dimensionless

n' ratio defined by Equation (28b), dimensionless

N_i number of perforations in i th propellant grains, dimensionless

$\bar{p}$ space-mean pressure resulting from burning i propellants, psi

p_b pressure on base of projectile, psi

p_g pressure of gas or air ahead of projectile, psi

p_i space-mean pressure resulting from burning of i th propellant, psi

p_I igniter pressure, psi

p_o breech pressure, psi

p_r resistance pressure, psi

Q energy released by burning propellant, in.-lb

r_i linear burning rate of i th propellant, in./sec

r'_i adjusted linear burning rate of i th propellant, in./sec

R_i functional relationship between r_i and $\bar{p}$

S_i surface area of partially burned i th propellant grain, $in.^2$

S_{g_i} surface area of an unburned i th propellant grain, $in.^2$

t time, sec

T mean temperature of propellant gases, ^oK

T_{o_i} adiabatic flame temperature of i th propellant, ^oK

T_{o_I} adiabatic flame temperature of igniter propellant, ^oK

T_S temperature of unburned solid propellant, ^oK

u_i two times the distance each surface of i th propellant grains has receded at a given time, in.

U internal energy of propellant gases, in.-lb

v velocity of projectile, in./sec

v_m velocity of projectile at muzzle of gun, in./sec

V specific volume of propellant gas, $in.^3/lb$

V_c volume behind projectile available for propellant gas, $in.^3$

V_{g_i} volume of an unburned i th propellant grain, $in.^3$

V_o volume of empty gun chamber, $in.^3$

W external work done on projectile, in.-lb

W_p weight of projectile, lb

x travel of projectile, in.

x_m travel of projectile when base reaches muzzle, in.

z_i fraction of mass of i th propellant burned, dimensionless

z_I fraction of mass of igniter burned, dimensionless

α_i burning rate exponent for i th propellant, dimensionless

β_i burning rate coefficient for i th propellant, $\frac{in.}{sec} - \frac{1}{psi^{\alpha}}$

γ' effective ratio of specific heats as defined by Equation (27a), dimensionless

γ_i ratio of specific heats for i th propellant, dimensionless

γ_I ratio of specific heats for igniter propellant, dimensionless

δ Pidduck-Kent constant, dimensionless

ρ_i density of i th solid propellant, $lb/in.^3$

INTRODUCTION

The interior ballistician must frequently predict the interior ballistic performance of guns. In some instances, it is sufficient to calculate muzzle velocity and maximum chamber pressure for a conventional gun from a knowledge of the propellant charge, the projectile weight, and the gun characteristics. This calculation is usually referred to as the classical central problem [1]* of interior ballistics. When non-conventional guns are considered or when detailed design information is required, it is necessary to know more than these two salient values. For the more demanding problems, complete interior ballistic trajectories may have to be calculated. These trajectories consist of displacement, velocity, and acceleration of the projectile and chamber pressure, all as functions of time.

The literature of interior ballistics contains descriptions of many methods for solving the problem of predicting the performance of guns. [1] [2] Methods, varying from the purely empirical to the "exact" theoretical, have been devised in tables, graphs, nomograms, slide rules, and simplified equations solved in closed-form. Some of these methods require data from the firing of the gun being considered or from a very similar gun. All of these methods require some simplification of the basic equations of interior ballistics.

To eliminate the restrictions imposed by assumptions made only to facilitate the mathematical solution of the problem, the interior ballistic equations have been programmed for high-speed electronic computers. Both analog and digital computers have been used to calculate detailed interior ballistic trajectories. There are advantages and disadvantages associated with each type of computer. Several years ago, [3] the interior ballistic equations were programmed for the digital computers** available here at the Ballistic Research Laboratories. Since that time, considerable use has been made of this program for studying gun and gun-like systems and for routine calculations.

---

* Superscripts indicate references listed at the end of this report.

** Although the interior ballistic equations were originally programmed only for the ORDVAC, [4] they have been recently reprogrammed in more general form [5] for the ORDVAC and the newer BRLESC. [4]

The computer program described in this report has been designed to solve a set of non-linear, ordinary differential and algebraic equations which simulate the interior ballistic performance of a gun. In this method, the usual set of equations which pertains to the burning of a single propellant has been modified to account for the burning of composite charges, i.e., charges made up of several propellants of different chemical compositions and different granulations.* The computer program may be suitably modified to study non-conventional guns and gun-like systems. A number of these optional programs have been devised and used extensively.**

INTERIOR BALLISTIC THEORY

Interior Ballistic System

The basic components of the interior ballistic system for a conventional gun are shown in Figure 1. A set of equations can be formulated which mathematically describes the distribution of energy originating from the burning

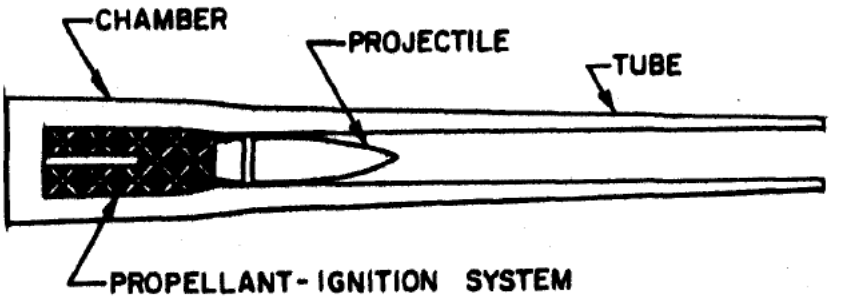

Figure 1. Basic Components of the Interior Ballistic System for a Conventional Gun

* The present program can be operated with as many as five different types of propellant charges for each problem.

** See Section entitled Options to Routine.

propellant and the subsequent motion of the components of the system. In the development which follows, two major assumptions are made to account for the behavior of composite charges:

1. The total chemical energy available is the simple sum of the chemical energies of the individual propellants.

2. The total gas pressure is the simple sum of the "partial pressures" resulting from the burning of the individual propellants.

Energy Equation

Application of the law of conservation of energy leads to the energy equation of interior ballistics. This may be written as:

$$\begin{matrix}\text{Energy Released} \\ \text{by Burning Propellant}\end{matrix} = \begin{matrix}\text{Internal Energy} \\ \text{of Propellant Gases}\end{matrix} + \begin{matrix}\text{External} \\ \text{Work Done} \\ \text{on Projectile}\end{matrix} + \begin{matrix}\text{Secondary} \\ \text{Energy Losses}\end{matrix} \qquad (1)$$

or:

$$Q = U + W + \text{Losses} \qquad (1a)$$

In Equation (1a) the energy released by the burning propellant (Q) is assumed to be equal to the simple sum of the energies released by the individual propellants as previously stated. Therefore:

$$Q = \sum_{i=1}^{n} \left[C_i z_i \int_0^{T_{o_i}} c_{v_i} \, dT \right] \qquad (2)$$

Because of gas expansion and external work performed in a gun, the gas temperature is less than the adiabatic flame temperature (T_{o_i}). The internal energy of the gas (U) is then:

$$U = \sum_{i=1}^{n} \left[C_i z_i \int_0^{T} c_{v_i} \, dT \right] \qquad (3)$$

The external work done on the projectile is given by:

$$W = A \int_0^{x} p_b \, dx \qquad (4)$$

Substituting Equations (2), (3), and (4) into Equation (1a) gives:

$$\sum_{i=1}^{n}\left[C_i z_i \int_0^{T_{o_i}} c_{v_i}\,dT\right] = \sum_{i=1}^{n}\left[C_i z_i \int_0^{T} c_{v_i}\,dT\right] + A\int_0^{x} p_b\,dx + \text{Losses}$$

which may be rewritten as:

$$\sum_{i=1}^{n}\left[C_i z_i \int_T^{T_{o_i}} c_{v_i}\,dT\right] = A\int_0^{x} p_b\,dx + \text{Losses} \tag{5}$$

As the c_{v_i} do not vary greatly over the temperature ranges from T to T_{o_i}, they can be replaced with mean values ($\bar{c}_{v_i}$). Integration of Equation (5) gives:

$$\sum_{i=1}^{n} C_i z_i \bar{c}_{v_i}\,(T_{o_i} - T) = A\int_0^{x} p_b\,dx + \text{Losses} \tag{6}$$

and solving for T:

$$T = \frac{\sum_{i=1}^{n} C_i z_i\ \bar{c}_{v_i}\ T_{o_i} - A\int_0^{x} p_b\,dx - \text{Losses}}{\sum_{i=1}^{n} C_i z_i\ \bar{c}_{v_i}} \tag{7}$$

Next, the "force" of each propellant is defined by:

$$F_i = m_i R T_{o_i} \tag{8}$$

and the well-known relations:

$$\bar{c}p_i - \bar{c}v_i = m_i R \tag{9}$$

and:

$$\gamma_i = \frac{\bar{c}_{p_i}}{\bar{c}_{v_i}} \tag{10}$$

are introduced.

Combination of Equations (9) and (10) gives:

$$\bar{c}_{v_i} (\gamma_i - 1) = m_i R \tag{11}$$

Substitution of Equation (11) into Equation (8) gives:

$$T_{o_i} = \frac{F_i}{(\gamma_i - 1)\, \bar{c}_{v_i}} \tag{12}$$

Finally, substitution of Equation (12) into Equation (7) gives Rèsal's equation in the form:

$$T = \frac{\sum_{i=1}^{n} \frac{F_i C_i z_i}{\gamma_i - 1} - A \int_0^x p_b \, dx - \text{Losses}}{\sum_{i=1}^{n} \frac{F_i C_i z_i}{(\gamma_i - 1)\, T_{o_i}}} \tag{13}$$

For most problems, it is convenient to assume the igniter completely burned ($z_I = 1$) at zero-time. Equation (13) may be restated as:

$$T = \frac{\left[\sum_{i=1}^{n} \frac{F_i C_i z_i}{\gamma_i - 1} \right] + \frac{F_I C_I}{\gamma_I - 1} - A \int_0^x p_b \, d_x - \text{Losses}}{\left[\sum_{i=1}^{n} \frac{F_i C_i z_i}{(\gamma_i - 1) T_{o_i}} \right] + \frac{F_I C_I}{(\gamma_I - 1)\, T_{o_I}}} \tag{14}$$

The terms $A \int_0^x p_b \, dx$ and Losses of Equation (14) can now be considered in more detail. The work done on the projectile results in an equivalent gain in kinetic energy of the projectile except for losses. Including these losses under the general category of energy losses:

$$A \int_0^x p_b \, dx = 1/2 \, \frac{W_P}{g} v^2 \tag{15}$$

According to Hunt, [2] the energy losses to be considered are:

(1) kinetic energy of propellant gas and unburned propellant,

(2) kinetic energy of recoiling parts of gun and carriage,

(3) heat energy lost to the gun,

(4) strain energy of the gun,

(5) energy lost in engraving the rotating band and in overcoming friction down the bore,

and

(6) rotational energy of the projectile.

For discussion of each type of secondary energy loss, see Reference (2). Types (2), (4), and (6) are estimated to be less than one percent for each category and have been neglected here.

The kinetic energy of propellant gas and unburned propellant can be represented by [6]

$$E_p = \frac{\left(\sum_{i=1}^{n} C_i\right) v^2}{2g\delta} \tag{16}$$

The energy losses resulting from heat lost to the gun can be estimated by a semi-empirical relationship described by Hunt:[2]

$$E_h = \frac{0.38c^{1.5}\left(x_m + \frac{V_o}{A}\right)\left(\frac{\sum_{i=1}^{n} C_i T_{o_i}}{\sum_{i=1}^{n} C_i} - T_\varepsilon\right) v^2}{\left[1 + \frac{0.6c^{2.175}}{\left(\sum_{i=1}^{n} C_i\right)^{0.8375}}\right] v_m^2} \tag{17}$$

At the present time, the introduction of a more sophisticated treatment of heat loss, with its attendant complexity, does not seem to be warranted. Such a substitution can be made if and when it appears desirable.

The final energy losses to be considered here consist of those resulting from engraving of the rotating band, friction between the moving projectile and the gun tube, and acceleration of air ahead of the projectile. Individual estimates of these are difficult to make, so they have been grouped as resistive pressure in the form:

$$E_{p_r} = A \int_0^x p_r \, dx \tag{18}$$

The p_r versus x function is discussed in greater detail in the section concerning forces acting on the projectile.

Substitution of Equations (15), (16), (17), and (18) into Equation (14) results in the form of the energy equation used in this computer program:

$$T = \frac{\left[\sum_{i=1}^{n} \frac{F_i C_i z_i}{\gamma_i - 1}\right] + \frac{F_I C_I}{\gamma_I - 1} - \frac{v^2}{2g}\left(W_p + \frac{\sum_{i=1}^{n} C_i}{\delta}\right) - A\int_o^x p_r \, dx - E_h}{\left[\sum_{i=1}^{n} \frac{F_i C_i z_i}{(\gamma_i - 1) T_{o_i}}\right] + \frac{F_I C_I}{(\gamma_I - 1) T_{o_I}}} \tag{19}$$

Equation of State

The pressure acting on the base of the projectile can be calculated from a series of equations, once the temperature of the gas is determined from the energy equation. Generally, the equation of state for an ideal gas takes the form:

$$p_i V_i = m_i RT \tag{20}$$

where V_i = the volume per unit mass of i th propellant gas.

Now, define V_c, the volume behind the projectile which is available for propellant gas, as:

Volume Available for Propellant Gas	=	Initial Empty Chamber Volume	+	Volume Resulting from Projectile Motion
	-	Volume Occupied by Unburned Solid Propellant	-	Volume Occupied by Gas Molecules (covolume)

(21)

or:
$$V_c = V_o + Ax - \sum_{i=1}^{n} \frac{C_i}{\rho_i} (1-z_i) - \sum_{i=1}^{n} C_i z_i b_i \tag{22}$$

By the definitions of Equations (20) and (21),

$$V_i = \frac{V_c}{C_i z_i} \tag{23}$$

Substituting Equations (8) and (23) into Equation (20) and rearranging gives:

$$p_i = \frac{F_i C_i z_i T}{V_c T_{o_i}} \tag{24}$$

If the b_i are assumed to be constants over the temperature range from T to T_{o_i}, and if the total gas pressure is taken as the simple sum of the "partial pressures" resulting from the burning of the individual propellants as previously stated, then:

$$\bar{p} = \sum_{i=1}^{n} p_i = \frac{T}{V_c} \sum_{i=1}^{n} \frac{F_i C_i z_i}{T_{o_i}} \tag{25}$$

As before, if it is assumed that the igniter is completely burned ($z_I = 1$) at zero-time, Equation (25) may be restated as:

$$\bar{p} = \frac{T}{V_c} \left[\left(\sum_{i=1}^{n} \frac{F_i C_i z_i}{T_{o_i}} \right) + \frac{F_I C_I}{T_{o_I}} \right] \tag{26}$$

The space-mean pressure, $\bar{p}$, given by Equation (26) is used in the calculation of the fraction of propellant burned at any time. This relationship is discussed in the section concerning burning rates. There is, however, a pressure gradient from the breech of the gun to the base of the projectile which must be considered in developing the equations of motion for the projectile. This pressure-gradient problem was first considered by Lagrange and is commonly referred to as the Lagrange Ballistic Problem. Later studies in this area were made by Love and Pidduck, [7] Kent, [8] and others. For this computer program, the improved Pidduck-Kent solution developed by Vinti and Kravitz [6] has been used:

$$p_b = \frac{\bar{p}}{1 + \frac{\sum_{i=1}^{n} C_i}{W_p \delta}} \qquad (27)^*$$

In addition the breech pressure, p_o, is calculated by the method contained in Reference (6). This is the pressure usually measured in experimental interior ballistic studies:

$$p_o = \frac{p_b}{(1-a_o)^{-n'-1}} \qquad (28)$$

$$\text{where: } 1/a_o = \frac{2n'+3}{\delta} + \frac{2(n'+1)}{\sum_{i=1}^{n} C_i/W_p} \qquad (28a)$$

---

* In Reference (6), the determination of δ depends on the ratio of specific heats, γ. For composite charges, an effective value is used for this purpose.

$$\gamma' = \frac{\sum_{i=1}^{n} C_i \gamma_i}{\sum_{i=1}^{n} C_i} \qquad (27a)$$

$$\text{and } n' = \frac{1}{\gamma' - 1} \tag{28b}$$

Mass-Fraction Burning Rate Equation

Both the energy equation (Equation (19)) and the equation of state (Equation (26)) are algebraic equations whose solutions depend upon the solutions of several non-linear, ordinary differential equations. The mass-fraction burning rate equation expresses the rate of consumption of solid propellant and hence the rate of evolution of propellant gas. This may be written as:

$$\frac{dz_i}{dt} = \frac{1}{V_{g_i}} S_i \; r_i \tag{29}$$

where: $$r_i = R_i \; (\bar{p}) \tag{30}$$

and: $$S_i = f_i \; (z_i) \tag{31}$$

For most gun propellants, Equation (30) may be quite satisfactorily stated as:

$$r_i = \beta_i (\bar{p})^{\alpha_i} \tag{32}$$

For certain propellants, including those plateau and mesa types used in solid-fuel rockets, Equation (32) will not suffice for gun calculations. In these cases, it is preferable to make use of a tabular listing of r_i's and corresponding $\bar{p}$'s (Equation (30)) and to interpolate for the desired r_i. The r_i's calculated by either Equation (30) or Equation (32) are closed chamber burning rates. As discussed in later sections of this report, these burning rates may be increased by addition of factors proportional to the velocity and displacement of the projectile in the following manner:

$$r_i' = r_i + K_v \, v + K_x \, x \tag{32a}$$

Similarly, the form function described by Equation (31) may be stated in one of several ways. In many interior ballistic systems, the form function is chosen for convenience of analytical solution. Where routine numerical computations are handled by use of a high-speed digital computer, the geometrical form of the propellant grain may be used to obtain the functional relationship, f_i, between S_i and z_i. For the usual grain shapes encountered, these equations are given in Appendix A. This Appendix also contains the method for handling such equations in the computer routine. To extend these equations to include propellant slivering see Reference (9).

Equations of Projectile Motion

The translational motion of the projectile down the gun tube may be calculated from the forces acting on the projectile. Figure 2 shows the axial forces considered in determining the resultant force.

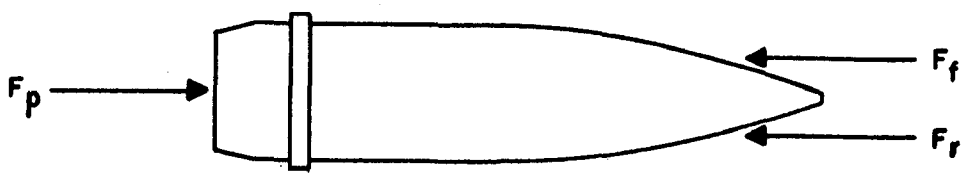

Figure 2. Axial Forces Acting on Projectile

The propulsive force, F_p, is that resulting from the pressure of the propellant gas on the base of the projectile according to:

$$F_p = p_b A \tag{33}$$

where p_b is obtained from Equation (27).

The frictional force, F_f, is the retarding force developed by resistance between the bearing surfaces of the projectile and the inside of the gun tube. This is usually the resistance between the rotating band and the rifling of the tube and includes the force required to engrave the rotating band. It may be expressed as:

$$F_f = p_r A \tag{34}$$

The determination of p_r is difficult in most cases. Many interior ballistic solutions use an increased projectile mass (approximately 5%) to account for its effect. There are several disadvantages inherent in such a treatment. Although the muzzle velocity may be calculated reasonably well, the detailed trajectory will be altered considerably. It is not possible to simulate the case where a projectile lodges in the bore (see Reference (10) for experimental trajectories for this condition). For this computer program, experimental data of the type given in Reference (11) may be used by inserting a tabulation of the function:

$$p_r = G(x) \tag{34a}$$

The gas retardation force, F_r, is that which results from the pressure of air or gas ahead of the projectile, stated as:

$$F_r = p_g A \tag{35}$$

where p_g is small enough to be neglected except for very high velocity systems, light gas guns, and other special applications. In the discussion of the Energy Equation in the Interior Ballistic Theory Section, p_g was considered a part of p_r.

The resultant force in the axial direction is then:

$$F_a = F_p - F_f - F_r \tag{36}$$

or:

$$F_a = A(p_b - p_g - p_r). \tag{37}$$

The acceleration of the projectile, by Newton's second law of motion, is:

$$a = \frac{A(p_b - p_g - p_r)}{M} \tag{38}$$

or:

$$a = \frac{Ag\,(p_b - p_g - p_r)}{W_p}. \tag{39}$$

Since $a = \frac{dv}{dt}$ and $v = \frac{dx}{dt}$, the velocity of the projectile is given by:

$$v = \int_0^t a \, dt \tag{40}$$

and the displacement of the projectile is given by:

$$x = \int_0^t v \, dt \tag{41}$$

Summary of Interior Ballistic Equations

The equations which are used in the computer program are now summarized for ease of reference.

Energy Equation

$$T = \frac{\left[\sum_{i=1}^{n} \frac{F_i C_i z_i}{\gamma_i - 1}\right] + \frac{F_I C_I}{\gamma_I - 1} - \frac{v^2}{2g}\left(W_p + \frac{\sum_{i=1}^{n} C_i}{\delta}\right) - A \int_0^x p_r \, dx - E_h}{\left[\sum_{i=1}^{n} \frac{F_i C_i z_i}{(\gamma_i - 1) T_{o_i}}\right] + \frac{F_I C_I}{(\gamma_I - 1) T_{o_I}}} \tag{19}$$

where:

$$E_h = \frac{0.38_c \, ^{1.5} \left(x_m + \frac{V_o}{A}\right) \left(\frac{\sum_{i=1}^{n} C_i T_{o_i}}{\sum_{i=1}^{n} C_i} - T_s\right) v^2}{\left[1 + \frac{0.6c \, ^{2.175}}{\left(\sum_{i=1}^{n} C_i\right) \, 0.8375}\right] v_m^2} \tag{17}$$

Equation of State

$$\bar{p} = \frac{T}{V_c} \left[\left(\sum_{i=1}^{n} \frac{F_i C_i z_i}{T_{o_i}} \right) + \frac{F_I C_I}{T_{o_I}} \right] \tag{26}$$

where: $$V_c = V_o + Ax - \sum_{i=1}^{n} \frac{C_i}{\rho_i} (1-z_i) - \sum_{i=1}^{n} C_i z_i b_i \tag{22}$$

$$p_b = \frac{\bar{p}}{1 + \frac{\sum_{i=1}^{n} C_i}{W_p \delta}} \tag{27}$$

$$p_o = \frac{p_b}{(1-a_o)^{-n'}-1} \tag{28}$$

Mass-Fraction Burning-Rate Equations

$$\frac{dz_i}{dt} = \frac{1}{V_{g_i}} S_i r_i \tag{29}$$

$$r_i = \beta_i (\bar{p})^{\alpha_i} \tag{32}$$

or:

$$r'_i = r_i + K_v v + K_x x \tag{32a}$$

Equations of Projectile Motion

$$a = \frac{Ag\,(p_b - p_g - p_r)}{W_p} \tag{39}$$

$$v = \int_0^t a\,dt \tag{40}$$

$$x = \int_0^t v\,dt \tag{41}$$

COMPUTATION ROUTINE

The set of non-linear, ordinary differential and algebraic equations, summarized at the end of the previous section, simulates the interior ballistic performance of a gun or gun-like system. A numerical computation routine has been devised for the simultaneous solution of these equations. The generalized flow-diagram for the routine is presented in Appendix B. Using the FORAST language, [5] the solution has been programmed for the ORDVAC and BRLESC computers.

Preliminary Routine

To reduce computation time and conserve memory space, a preliminary routine has been introduced. Here all data required for the computation are read into the computer, constant groupings (e.g.,

$$\frac{F_i C_i}{(\gamma_i - 1)\,T_{o_i}}\,,\quad \frac{F_i C_i}{(\gamma_i - 1)}\,,\quad \frac{C_i}{\rho_i}\,,\ \text{etc.,}$$

are calculated and stored for subsequent use, and data to permanently identify the computer run are printed out. A complete listing of required input data may be found in Appendix C.

Main Routine

The main computational routine is presented in the generalized flow-diagram of Appendix B. To follow the procedure, consider the three sequential phases of the problem:

Phase I - From time of ignition until the projectile starts to move.

Phase II - From time of initial projectile motion until all propellants are consumed.

Phase III - From time of propellant burnout until projectile leaves the gun muzzle.

At the time of ignition (Phase I begins), it is assumed that the igniter is completely burned ($z_I = 1$) and none of the other propellants have started to burn (all $z_i = 0$). The space-mean pressure, consisting only of the igniter pressure, is calculated from:

$$\bar{p} = p_I = \frac{F_I C_I}{V_c} \tag{42}$$

Equation (42) is derived from Equations (19) and (26) by means of the simplifying ignition assumptions stated above.

The linear burning rate for each propellant can now be determined from either Equation (30) or Equation (32) in combination with Equation (32a). If the interpolation indicated by use of Equation (30) is selected, the generalized interpolation sub-routine* is employed. The mass-fractions burned, z_i's, during a small time interval, dt, are determined by integration of Equation (29). The surface areas of the unburned propellant (see Appendix A) are used in this initial calculation. The Runga-Kutta method of numerical integration, as modified by Gill, [12] is commonly used for the solution of sets of ordinary differential equations and has been employed here.

Calculation of the temperature, T, from Equation (19) and the volume available for propellant gas, V_c, from Equation (22), will allow the calculation of the new space-mean pressure, $\bar{p}$, at time, dt, from Equation (26). The surface areas of the now partially burned propellants are computed from equations presented in Appendix A. All results of interest are printed-out at this time ** and these results used as initial conditions for calculations during

* See Reference (18) for interpolation by divided differences.

** See Appendix C for listing of output data.

the ensuing time-interval. Those terms in Equations (17), (19), and (22) which involve velocity or displacement are zero during this phase of the computation. This calculation-loop is continued until the space-mean pressure exceeds a pre-selected "shot-start" pressure and the projectile starts to move. Phase I, which has been arbitrarily defined, ends at this time.

Phase II requires the addition of the equations of motion to the sequence followed during Phase I. Equations (27), (39), (40), and (41) are used to calculate the values of the acceleration, velocity, and displacement of the projectile at the end of each time interval. Integration specified in Equations (40) and (41) is again performed by the Runga-Kutta-Gill method. Values of velocity and displacement are now available for use in terms of Equations (17), (19), and (22). To compute values for $E_{p_r} = A \int_0^x p_r \, dx$, which is one of the terms in Equation (19), the generalized interpolation sub-routine must be used to obtain p_r from the tabular information described by Equation (34a). This integration is performed by use of the Trapezoidal Rule.*

As time is increased by the addition of small time-intervals, calculations during Phase II are continued around this expanded loop with print-out of appropriate results at the end of each time interval. One at a time, the propellants are completely consumed and this phase is ended. A series of switches has been incorporated in the program to circumvent the necessity of introducing propellants in any special order. In fact, it may not always be possible to predict the exact order in which several different propellants will be burned out. The combination of the propellant switches and the start-of-motion switch makes it possible to handle problems where one or more propellants burn out before the projectile starts to move.

With all propellants consumed, Phase III begins. The mass-fractions burned have all become unity and the equations concerned with burning (Equations (29), (31), and (30) or (32)) are eliminated from the loop. As in the other phases,

---

* Although the Trapezoidal Rule is a relatively crude method for numerical integration, the accuracy of the p_r versus x data available does not warrant a more accurate and hence more complex method.

results are printed-out at the end of each time-interval. A continual check is made of the displacement of the projectile to determine whether or not it has reached the muzzle of the gun. When the projectile passes the muzzle, Phase III has ended and the program is stopped.

It is possible for the projectile to reach the muzzle (and the program stopped) before Phase II is completed. This would simulate a gun-firing in which unburned propellant is ejected from the muzzle. It is also possible for the program to simulate a firing in which the projectile becomes lodged in the tube. In this case, Phase III is not completed and the program is stopped when the projectile displacement does not increase.

At each time-interval after the beginning of Phase II, the breech pressure is determined from Equation (28) and printed out. This result is not used in the computational routine but is used to compare theoretical and experimental results. A continual check is made of the calculated pressures and the maximum breech pressure is stored with its associated time and projectile displacement. This information is printed-out at the end of the program. Calculations during the last time-interval result in a projectile displacement somewhat greater than the desired distance to the muzzle. A linear interpolation between results at the last two time-intervals is used to obtain results exactly at the muzzle. These results are also printed-out at the end of the program.

Options to Routine

A considerable number of options have been designed and coded for special problems. These include changes which enable the program to be used for guns, or gun-like weapons, which are not of conventional design (Figure 1) and changes which vary the treatment of some of the individual parameters. It is expected that the number of such options will increase as the program is used for a greater number and variety of problems.

Typical options for non-conventional guns are those for gun-boosted rockets, traveling-charge guns, and light-gas guns of the adiabatic compressor type. Examples of options for varied treatment of individual parameters are those for adjusted burning rates (previously mentioned), inhibited propellant surfaces, delayed propellant ignition, variable time-intervals, constant resistive pressure, and resistive pressure as a function of base pressure.

DISCUSSION

No attempt has been made here to present a new and different interior ballistic theory. The objective was to devise a convenient, flexible scheme for performing the tedious numerical calculations required to obtain detailed interior ballistic trajectories. The selection of a program for high-speed digital computers has made it possible to eliminate most of the simplifications of theory required to facilitate mathematical solutions by other methods.

The theory presented as the basis for the computer routine is well-known and has only been modified to account for composite charges. There are several problems present in all interior ballistic calculations and these also prove troublesome here. For example, useful propellant burning rates are not generally available. It is known that burning rates obtained from experimental firings in closed chambers are usually low. The results obtained from limited gun-firings by the authors [11] indicate gun burning rates may be twice closed chamber burning rates under certain conditions. As previously mentioned, optional methods of adjusting closed chamber burning rates have been provided for in this program. One such approach is to consider the burning rate to be a function of the projectile velocity (and possibly a function of the projectile displacement) in addition to its known dependence on pressure. This method results in the use of closed chamber burning rates when the gun chamber is practically a closed chamber (v and x are effectively zero). When the projectile is moving at higher velocities and is further down tube, reasonable increases in burning rates are obtained and used. Other equally important difficulties are associated with the determination of reasonable values for resistive pressure and shot-start pressure.

Considerable versatility has been built into the program. Instead of stopping the computation at the end of Phase III, a new problem can be automatically read into the computer and solved. This multiple-case feature can be employed to advantage for any number of additional problems during a single computer run.

Typical interior ballistic problems were used to compare results obtained from this computer routine with results from other interior ballistic schemes. (13), (14), and (15). The agreement was generally very good when the other

schemes were fairly sophisticated. In addition, detailed interior ballistic trajectories are produced in considerably less time than it takes to calculate maximum pressure and muzzle velocity by other systems. A typical computer solution for a conventional gun takes only 10 seconds if magnetic tape output is used with the BRLESC.

Results from computer simulations have also been compared to experimental data obtained from well-instrumented gun firings. To demonstrate the adequacy of the computer routine, data from a typical 105mm Howitzer firing were processed by the method described in Reference (11). In Appendix D these experimental results are compared with the predicted results obtained from a simulation of this firing.

Paul G. Baer

PAUL G. BAER

Jerome M. Frankle

JEROME M. FRANKLE

LIST OF REFERENCES

1. Corner, J. Theory of the Interior Ballistics of Guns. New York: John Wiley and Sons, Inc., 1950.

2. Hunt, F. R. W. Chairman, Editorial Panel. Internal Ballistics. New York: Philosophical Library, 1951.

3. Baer, Paul G., and Frankle, Jerome M. Digital Computer Simulation of the Interior Ballistic Performance of Guns. Ordnance Computer Research Report, VI, No. 2: 17-23, Aberdeen Proving Ground, Apr 1959.

4. Kempf, Karl, Historical Officer. Historical Monograph - Electronic Computers within the Ordnance Corps. Aberdeen Proving Ground, Nov 1961.

5. Campbell, Lloyd W., and Beck, Glenn A. The FORAST Programming Language for ORDVAC and BRLESC. Aberdeen Proving Ground: BRL R-1172, Aug 1962.

6. Vinti, John P., and Kravitz, Sidney. Tables for the Pidduck-Kent Special Solution for the Motion of the Powder Gas in a Gun. Aberdeen Proving Ground: BRL R-693, Jan 1949.

7. Love, A. E. H., and Pidduck, F. B. The Lagrange Ballistic Problem. Phil. Trans. Roy. Soc. 222: 167, London, 1923.

8. Kent, R. H. Some Special Solutions for the Motion of the Powder Gas. Physics, VII, No. 9: 319, 1936.

9. Frankle, Jerome M., and Hudson, James R. Propellant Surface Area Calculations for Interior Ballistic Systems. Aberdeen Proving Ground: BRL M-1187, Jan 1959.

10. Frankle, Jerome M. Special Interior Ballistic Tests of 115mm XM378 Slug Rounds. Aberdeen Proving Ground: BRL M-1266, May 1960 (Confidential).

11. Baer, Paul G., and Frankle, Jerome M. Reduction of Interior Ballistic Data from Artillery Weapons by High-Speed Digital Computer. Aberdeen Proving Ground: BRL M-1148, Jun 1958.

12. Gill, S. Runge-Kutta-Gill Numerical Procedure for Solving Systems of First Order Ordinary Differential Equations. Proceedings of the Cambridge Philosophical Society, 47, Part I: 96, Jan 1951.

13. Hitchcock, Henry P. Tables for Interior Ballistics. Aberdeen Proving Ground: BRL R-993, Sep 1956 and BRL TN-1298, Feb 1960.

14. Taylor, W. C., and Yagi, F. A Method for Computing Interior Ballistic Trajectories in Guns for Charges of Arbitrarily Varying Burning Surface. Aberdeen Proving Ground: BRL R-1125, Feb 1961.

15. Strittmater, R. C. A Single Chart System of Interior Ballistics. Aberdeen Proving Ground: BRL R-1126, Mar 1961.

16. Scarborough, James B. Numerical Mathematical Analysis. Baltimore: The Johns Hopkins Press, 2nd ed., 1950.

17. Baer, Paul G., and Bryson, Kenneth R. Tables of Computed Thermodynamic Properties of Military Gun Propellants. Aberdeen Proving Ground: BRL M-1338, Mar 1961.

18. Milne, William Edmund. Numerical Calculus. Princeton, New Jersey: Princeton University Press, 1949.

APPENDICES

A. FORM FUNCTION EQUATIONS

B. COMPUTATION ROUTINE

C. INPUT AND OUTPUT DATA

D. COMPARISON OF EXPERIMENTAL AND PREDICTED PERFORMANCE FOR TYPICAL 105MM HOWITZER FIRING

APPENDIX A

Form Function Equations

FORM FUNCTION EQUATIONS

Geometrical Equations

1. Initial Volume of a Propellant Grain

$$V_{g_i} = \frac{\pi}{4} (D_i^2 - N_i d_i^2) L \qquad \text{(A-1)}$$

where: V_{g_i} = volume of an unburned propellant grain, in.^{3}

D_i = outside diameter of grain, in.

N_i = number of perforations, dimensionless

d_i = diameter of perforation, in.

L_i = length of grain, in.

2. Volume of a Partially Burned Propellant Grain

$$V_{g_i}(1 - z_i) = \frac{\pi}{4} \left[(D_i - u_i)^2 - N_i (d_i + u_i)^2 \right] (L_i - u_i) \qquad \text{(A-2)}$$

where: z_i = mass-fraction of i th propellant burned at a given time, dimensionless

u_i = two times the distance each surface has receded at a given time, in.

3. Initial Surface Area of a Propellant Grain

$$S_{g_i} = \pi \left[(D_i + N_i d_i)(L_i) + \frac{D_i^2 - N_i d_i^2}{2} \right] \qquad \text{(A-3)}$$

where: S_{g_i} = surface area of an unburned propellant grain, in.^{2}

4. Surface Area of a Partially Burned Propellant Grain

$$S_i = \pi \left\{ \left[(D_i - u_i) + N_i (d_i + u_i) \right] \left[L_i - u_i \right] + \frac{(D_i - u_i)^2}{2} - \frac{N_i (d_i + u_i)^2}{2} \right\} \qquad \text{(A-4)}$$

where: S_i = surface area of partially burned i th propellant grain at a given time, in.^{2}.

Equations for Newton-Raphson Method* for Finding Approximate Values of the Real Roots of a Numerical Equation

1. Rearrange Equation (A-2) to set $f(u_i) = 0$:

$$f(u_i) = \frac{\pi}{4}\left\{(N_i-1)\,u_i^3 - \left[L_i(N_i-1) - 2(D_i+N_i d_i)\right] u_i^2 - \left[2L_i(D_i + N_i d_i) + (D_i^2 - N_i d_i^2)\right] u_i + L_i\,(D_i^2 - N_i d_i^2)\right\} - V_{g_i}\,(1-z_i) \qquad \text{(A-5)}$$

2. Differentiate Equation (A-5) with respect to u_i:

$$f'(u_i) = \frac{d\left[f(u_i)\right]}{du_i} = \frac{\pi}{4}\left\{3(N_i-1)u_i^2 - 2\left[L_i(N_i-1) - 2\,(D_i + N_i d_i)\right] u_i - \left[2L_i(D_i+N_i d_i) + (D_i^2 - N_i d_i^2)\right]\right\} \qquad \text{(A-6)}$$

3. The value of the root of Equation (A-2) is then:

$$u_{i+1} = u_i - \frac{f(u_i)}{f'(u_i)} \qquad \text{(A-7)}$$

where: u_{i+1} = the improved value of the root, where the first estimate of the root is u_i.

Procedure

1. For each propellant, determine z_i by integration of Equation (29). In the initial calculation of each z_i, Equation (A-3) is used to compute each S_i ($S_i = S_{g_i}$ when $u_i = 0$). For subsequent calculations of each z_i, Equation (A-4) is used with u_i determined as described below.

* See Reference (16) for a discussion of this method.

2. The z_i's obtained from Equation (29) are used to compute the u_i's from Equation (A-7) and then the new S_i's are computed from Equation (A-4). In the initial calculation of u_i, the first estimate of its value is zero.

Equation (A-7) is used to calculate the improved value, u_{i+1}. With u_{i+1} as the estimate, Equation (A-7) is used again to calculate a further-improved value, u_{i+2}. This procedure is continued until the improvement is less than 10^{-5} inch.

APPENDIX B

Computation Routine

1. Generalized Flow Diagram
2. FORAST Listing

INTERIOR BALLISTICS PROGRAM FOR GUNS
GENERALIZED FLOW DIAGRAM

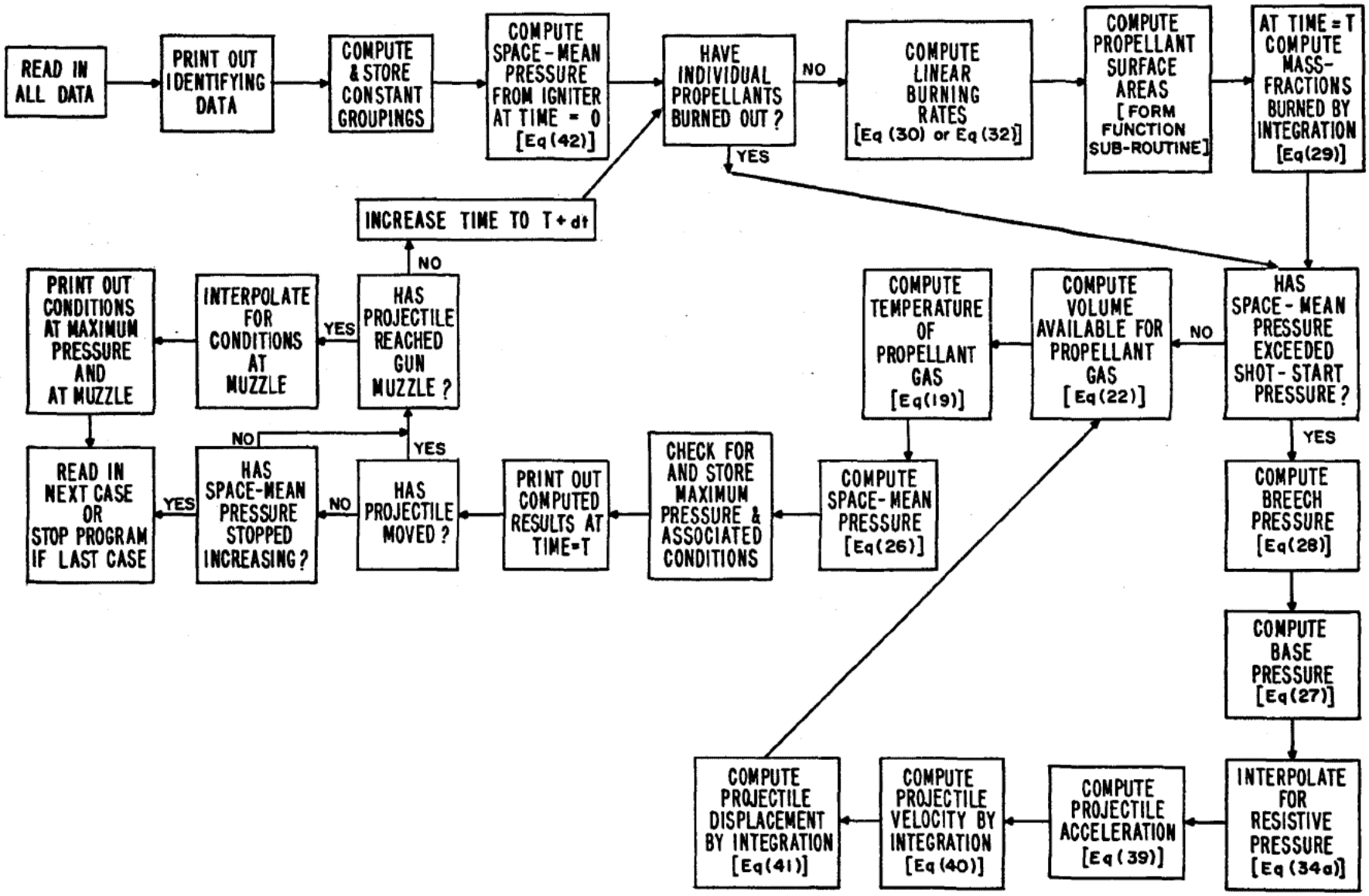

```
PROB 1 664MG  MULTI-GRAN GUN BALLISTICS
      BLOC(PR1-PR20)          AC1-AC5)K1-K7)Y1-Y7)T1-T5)U0-U5)S1-S5)R1-R5)          0003
      BLOC(BC1-BC5)CC1-CC5)DC1-DC5)EC1-EC5)GC1-GC5)IC1-IC5)JC1-JC5)FC1-FC5)          0004
      BLOC(Q1-Q7)C1-C5)F1-F5)GA1-GA5)COV1-COV5)TO1-TO5)RHO1-RHO5)BET1-BET5)          0005
      BLOC(DCZ1-DCZ5)AN1-AN104)                                                     1  5
      CONTALP1-ALP5)D1-D5)(DP1-DP5)L1-L5)NP1-NP5)XC1-XC20)HC1-HC5)                  0006
B1        ENTER(A,READ)AN1)13)%                                                      7
          READ-FORMAT(01)-(WP)XM)V0)AP)PE)DEL)PPMAX)%                                8
          READ-FORMAT(01)-(CI)FI)GAI)TOI)%                                        1008
          READ-FORMAT(01)-(DT)N1)KV)KX)D)EVP)% SET(J=0)%                             9
B1.1      READ-FORMAT(01)-(XC1,J)PR1,J)% COUNT(20)IN(J)GOTO(B1.1)%                  10
          ENTER(INTEGER)N1)N)%SET( J=0)% INT(NCP=-2*N)%                           0011
B2        READ-FORMAT(01)-(C1,J)F1,J)GA1,J)COV1,J)TO1,J)RHO1,J)%                    12
          READ-FORMAT(01)-(BET1,J)ALP1,J)D1,J)DP1,J)L1,J)NP1,J)%                  1012
                    COUNT(,N)IN(J)GOTO(B2)%SET(J=0)%                              0013
B2.1      ENTER(A,PUNCH)AN1)1)% ENTER(A,PUNCH)AN89)1)%                               14
          ENTER(A,PUNCH)AN9)1)%                                                      15
          PUNCH-FORMAT(02)-<1>(WP)XM)V0)AP)DEL)PE)PPMAX)<Δ>%                         16
          ENTER(A,PUNCH)AN89)1)% ENTER(A,PUNCH)AN17)2)%                              17
          PUNCH-FORMAT(03)-<1>(CI)FI)GAI)TOI)<IGNITERΔ>%                          1017
B3        PUNCH-FORMAT(04)-<1>(C1,J)F1,J)GA1,J)COV1,J)TO1,J)RHO1,J)<Δ>%              18
          COUNT(,N)IN(J)GOTO(B3)% SET(J=0)% ENTER(A,PUNCH)AN89)1)%                   19
          ENTER(A,PUNCH)AN33)1)%                                                     20
B3.1      PUNCH-FORMAT(05)-<1>(BET1,J)ALP1,J)D1,J)DP1,J)L1,J)NP1,J)<Δ>%              21
          COUNT(,N)IN(J)GOTO(B3.1)% SET(J=0)% ENTER(A,PUNCH)AN89)1)%                 22
          ENTER(A,PUNCH)AN41)2)%                                                     23
B3.2      PUNCH-FORMAT(06)-<1>(XC1,J)PR1,J)<Δ>%                                      24
          COUNT(20)IN(J)GOTO(B3.2)% SET(J=0)% ENTER(A,PUNCH)AN89)1)%                 25
          ENTER(A,PUNCH)AN57)2)% SET(SWP=B18.1)JP=0)STUCK=B18.5)%                    26
          PUNCH-FORMAT(07)-<1>(DT)N1)KV)KX)EVP)D)<Δ>%                                27
B4        BC1=FI*CI/(GAI-1)% AC1=BC1/TOI%CC1=FI*CI/TOI% EVM=EVP*12%                0035
B4.1      BC1,J=F1,J*C1,J/(GA1,J-1)% AC1,J=BC1,J/TO1,J% CC1,J=F1,J*C1,J/           0036
      CONTTO1,J%                                                                   0037
          DC1,J=C1,J/RHO1,J% EC1,J=C1,J*COV1,J% FC1,J=NP1,J-1%                     0038
          GC1,J=L1,J(NP1,J-1)-2(D1,J+NP1,J*DP1,J)%                                 0039
          HC1,J=2*L1,J(D1,J+NP1,J*DP1,J)+(D1,J**2-NP1,J*DP1,J**2)%                 0040
          IC1,J=L1,J(D1,J**2-NP1,J*DP1,J**2)%                                      0041
          JC1,J=3.1416*IC1,J/4%COUNT(,N)IN(J)GOTO(B4.1)%SET(J=0)%                  0042
B5        CT=0%TP1=0%                                                              0043
B5.1      TP1=C1,J*GA1,J+TP1% CT=C1,J+CT% COUNT(,N)IN(J)GOTO(B5.1)%                0044
          GAP=TP1/CT%SET(J=0)%GAF=GAP/(GAP-1)%EP=CT/WP%                            0045
          EP1=1+EP/DEL%TP1=1/(GAP-1)%TP2=1/((2*TP1+3)/DEL+(2*TP1+2)/EP)%           0046
          MCTD=WP*CT/DEL%TP4=0%AGW=AP*386.4/WP%                                    0047
          EP2=EXP(GAF*LOG(1-TP2))% TP1=EXP(1.5*LOG(D))% TP2=EXP(2.175*LOG          0048
      CONT(D))%                                                                    0049
          TP3=EXP(.8375*LOG(CT))%                                                  0050
B5.2      TP4=C1,J*TO1,J+TP4% COUNT(,N)IN(J)GOTO(B5.2)% SET(J=0)%                  0051
          HCL=(.38*12*TP1(XM+V0/AP)(TP4/CT-298))/((1+0.6*TP2/TP3)                  0052
      CONTEVM**2)%                                                                 0053
B6        CLEAR(7)NOS.AT(K1)% CLEAR(7)NOS.AT(Y1)% CLEAR(7)NOS.AT(Q1)%              0054
          PB=PR=PBR=XI=ALP=INTPR=0% T=DT%                                            55
          CLEAR(5)NOS.AT(U1)%  XLST=0%  PRLST=0%                                   0056
B6.1      Y3,J=1.1% COUNT(5)IN(J)GOTO(B6.1)% SET(J=0)%                             0057
B6.2      Y3,J=0% COUNT(,N)IN(J)GOTO(B6.2)% SET(J=0)%                              0058
B7.1      IF-INT(N=1)GOTO(B7.5)%  SET(SW3=DR3.1)%                                  0059
          IF-INT(N=2)GOTO(B7.6)%  SET(SW4=DR3.1)%                                    6
          IF-INT(N=3)GOTO(B7.7)%  SET(SW5=DR3.1)%                                  0061
          IF-INT(N=4)GOTO(B7.8)%  SET(SW6=DR3.1)% GOTO(B8)%                        0062
```

```
B7.5    SET(SW3=B14)%GOTO(B8)%                                                  0063
B7.6    SET(SW4=B14)%GOTO(B8)%                                                  0064
B7.7    SET(SW5=B14)%GOTO(B8)%                                                  0065
B7.8    SET(SW6=B14)%GOTO(B8)%                                                  0066
B8      TP1=0%                                                                  0067
B8.1    TP1=DC1,J+TP1%  COUNT(,N)IN(J)GOTO(B8.1)%  SET(J=0)%                    0068
        PT=CI*FI/(V0-TP1)% SET(SW1=B15)SW8=B14.5)% PMAX=PT%                      0069
        ENTER(R,K,G,)DT)2,N)B9)Y1)K1)Q1)% GOTO(,SW1)%                           0070
B9      IF(Y3>=1)GOTO(B9.1)%SET(SW11=B10)J=0)%GOTO(DR1)%                        0071
B9.1    Y3=1%K3=0%S1=0%R1=0%Q3=0%SET(SW11=B10)J=0)%GOTO(DR3.1)%                  72
B10     IF(Y4)=1)GOTO(B10.1)%SET(SW11=B11)J=1)%GOTO(DR1)%                       0073
B10.1   Y4=1%K4=0%S2=0%R2=0%Q4=0%SET(SW11=B11)J=1)%GOTO(,SW3)%                    74
B11     IF(Y5>=1)GOTO(B11.1)%SET(SW11=B12)J=2)%GOTO(DR1)%                       0075
B11.1   Y5=1%K5=0%S3=0%R3=0%Q5=0%SET(SW11=B12)J=2)%GOTO(,SW4)%                    76
B12     IF(Y6>=1)GOTO(B12.1)%SET(SW11=B13)J=3)%GOTO(DR1)%                       0077
B12.1   Y6=1%K6=0%S4=0%R4=0%Q6=0%SET(SW11=B13)J=3)%GOTO(,SW5)%                    78
B13     IF(Y7>=1)GOTO(B13.1)%SET(SW11=B14)J=4)%GOTO(DR1)%                       0079
B13.1   Y7=1%K7=0%S5=0%R5=0%Q7=0%SET(SW11=B14)J=4)%GOTO(,SW6)%                    80
B14     SET(J=0)%TP1=0%                                                         0081
B14.1   TP1=DC1,J(1-Y3,J)+EC1,J*Y3,J+TP1%COUNT(,N)IN(J)GOTO(B14.1)%             0082
        VC=V0+AP*XI-TP1%SET(J=0)%TP1=BC1%                                       0083
B14.2   TP1=BC1,J*Y3,J+TP1%COUNT(,N)IN(J)GOTO(B14.2)%                           0084
        SET(J=0)%TP2=AC1%                                                       0085
B14.3   TP2=AC1,J*Y3,J+TP2%COUNT(,N)IN(J)GOTO(B14.3)%                           0086
        SET(J=0)%TEMP=(TP1-ALP)/TP2%TP1=CC1%                                    0087
B14.4   TP1=CC1,J*Y3,J+TP1%COUNT(,N)IN(J)GOTO(B14.4)%                           0088
        SET(J=0)%PT=TEMP*TP1/VC%                          GOTO(,SW8)%           0089
B14.5   ENTER(R,K,GD)%                                                          0090
DR1     R1,J=BET1,J+EXP(ALP1,J*LOG(PT))%U0=U1,J%H1=FC1,J%H2=GC1,J%              0092
        H3=HC1,J%H4=IC1,J%H5=JC1,J(1-Y3,J)%H6=L1,J%H7=D1,J%                      0093
        H8=DP1,J%H9=NP1,J%H10=DC1,J%H11=JC1,J%GOTO(GAM2)%                       0094
DR3     R1,J=R1,J+KV*K2+KX*XI%                                                  1094
        K3,J=S1,J+R1,J/DC1,J%                                                     95
DR3.1   GOTO(,SW11)%                                                            1095
DR4     PB=PT/EP1%PBR=PB/EP2%                                                   0096
        K1=AGW(PB-PR)%K2=Y1%XI=Y2%                                              0097
        IF(XI<XC20)GOTO(DR5)% PR=PR20% GOTO(DR9)%                               0099
DR5     ENTER(D,D,IN)XI)PR)XC1)PR1)20)3)1))%                                    0100
DR9         DELX=XI-XLST%SUM1=PR+PRLST%                                         0098
        INTPR=(DELX*SUM1)/2+INTPR%XLST=XI%PRLST=PR%                             0099
        ALP=(MGTD*K2**2/772.8)+AP*INTPR+HCL*K2**2% GOTO(B14.5)%                 0100
B15     IF(PT<PE)GOTO(B15.1)% SET(SW8=DR4)SW1=B16)%                             0101
B15.1   PBR=PT% PB=PT%                                                          0102
B16     IF(Y1>0)GOTO(B17)%IF(Y3>=1)AND(Y4>=1)AND(Y5>=1)AND(Y6>=1)                103
    CONTAND(Y7>=1)GOTO(B16.1)%GOTO(B17)%                                        1103
B16.1   SET(STUCK=B22)%                                                         2103
B17     XF=XI/12%V=Y1/12%AF=K1/12%SET(J=0)%ST=0%                                0104
B17.1   DCZ1,J=K3,J*C1,J%COUNT(,N)IN(J)GOTO(B17.1)%SET(J=0)%                    0105
B17.2   ST=S1,J+ST%COUNT(,N)IN(J)GOTO(B17.2)%SET(J=0)%                          0106
        IF(PBR<PPMAX)GOTO(B17.3)% ENTER(A,PUNCH)AN73)1)% GOTO(NEWRN)%           1106
B17.3   IF(PMAX>PBR)GOTO(B18)% PMAX=PBR% XPMAX=XI% TPMAX=T%                     107
B18     GOTO(,SWP)%                                                             108
B18.1   ENTER(A,PUNCH)AN1)1)%                                                   109
B18.2   ENTER(A,PUNCH)AN89)1)% TM=T*1000%                                       110
        PUNCH-FORMAT(08)-<1>(TM)XI)PBR)PT)PB)V)AF )<Δ>%                         111
        PUNCH-FORMAT(09)-<1>(TM)XI)XF)TEMP)VC)PR)ST)<Δ>%                        112
B18.3   PUNCH-FORMAT(010)-<1>(TM)XI)Y3,J)DCZ1,J)R1,J)S1,J)<Δ>%                  1112
        COUNT(,N)IN(J)GOTO(B18.3)% SET(J=0)%                                    2112
```

```
         COUNT(15,NCP)IN(JP)GOTO(B18.4)% SET(SWP=B18.1)JP=0)GOTO(.STUCK)%  3112
B18.4    SET(SWP=B18.2)%GOTO(.STUCK)                                      4112
B18.5    T=T+DT%                                                           113
         IF(XI>XM)GOTO(B21)%XILST=XI%VLST=V%PRLST=PB%                     0114
         ENTER(R,K,G1)%                                                   0115
B21      VMAX=((XM-XILST)(V-VLST)/(XI-XILST))+VLST%                       0116
         PBMAX=((XM-XILST)(PB-PBLST)/(XI-XILST))+PBLST%                   0117
         TPMAX=TPMAX*1000%                                                1117
         ENTER(A,PUNCH)AN89)1)% ENTER(A,PUNCH)AN81)1)%                     118
         PUNCH-FORMAT(011)-<1>(VMAX)PMAX)XPMAX)TPMAX)PBMAX)<Δ>%            119
         GOTO(NEWRN)%                                                     1119
B22      ENTER(A,PUNCH)AN89)1)%ENTER(A,PUNCH)AN97)1)%ENTER(A,PUNCH)AN81)1)% 120
         VMAX=0%PBMAX=0%TPMAX=TPMAX*1000%                                  121
         PUNCH-FORMAT(011)-<1>(VMAX)PMAX)XPMAX)TPMAX)PBMAX)<Δ>%            122
NEWRN    GOTO(B1)%                                                         123
GAM2     T1=H7-U0%T2=H8+U0                                                0127
FF1.1    FU=.7854(U0**3*H1-U0**2*H2-U0*H3*H4)-H5%                         0128
FF2      FPU=.7854(3*U0**2*H1-2*U0*H2-H3)%                                0129
FF2.1    U01=U0-FU/FPU%                                                   0130
FF3      IF-ABS((U01-U0)<=.00001)GOTO(FF4)%U0=U01%                        0131
FF3.1    GOTO(GAM2)%                                                      0132
FF4      SI=3.1416((H6-U0)(H7-U0+H9(H8+U0))+.5*T1**2-.5*H9                0133
     CONT*T2**2)%S1,J=SI*H10/H11%U1,J=U0%GOTO(DR3)%                       0134
01       FORM(10-10)1-7)                                                   132
02       FORM(12-2-9)1-1)12-3-10)1-3)3-2)12-1-8)3-1)12-6-8)3-3)12-6-8-9)   133
03       FORM(12-2-9)12-7-9)3-2)12-1-7)3-13)12-4-6-25)                     134
04       FORM(12-2-9)12-7-9)3-2)12-1-7)3-4)12-2-7)3-2)12-4-6)3-4)12-0-8-20) 135
05       FORM(12-9)3-1)12-6)3-4)12-6)3-4)12-6)3-4)12-1-7)3-5)12-1-3-23)    136
06       FORM(3-20)12-3-8)3-11)12-5-7-32)                                  137
07       FORM(12-7)3-5)12-1-3)3-4)12-9)3-1)12-9)3-5)12-4-6)3-5)12-1-7-17)  138
08       FORM(12-2-8)3-1)12-3-8)3-2)12-6-10)12-6-10)12-6-10)12-5-9)3-1)    139
     CONT12-4-10-9)                                                       1139
09       FORM(12-2-8)3-1)12-3-8)3-2)12-2-8)3-2)12-4-8)3-2)12-5-10)12-4-7)3-3) 140
     CONT12-5-9-10)                                                       1140
010      FORM(12-2-8)3-1)12-3-8)3-2)12-1-7)3-3)12-4-9)3-1)12-3-8)3-2)12-5-9-20) 141
011      FORM(12-5-8)3-5)12-6-8)3-4)12-3-8)3-2)12-2-7)3-3)12-6-9-24)       142
         END GOTO(B1)%                                                    0148
8                                  105 MM HOWITZER    RD 765                Δ
1PROJ. WT.   BARREL   CHAMBER  BORE AREA     P-K     SS PRESS MAX GUN PRESSURE Δ
1                                  M1 PROPELLANT                           Δ
1 CHARGE     FORCE      GAMMA     COVOLUME FLAME TEMP  DENSITY             Δ
1  BETA      ALPHA   O.D. GRAIN DIA. PERF GR.LENGTH NO. PERF.               Δ
1                                  RESISTANCE                              Δ
1                      PROJ. TRAVEL          PRESSURE                      Δ
1                                  MISCELLANEOUS                           Δ
1   DT     NO. PROP.      KV          KX     EST. MUZ. VEL. DIAMETER       Δ
1                     P GREATER THAN DESIRED MAX PRESSURE                  Δ
1MUZZLE VEL. MAX. PRESSURE X AT PMAX T AT PMAX MUZ PRESSURE                Δ
1                                                                          Δ
1                                  PROJECTILE STOPPED                      Δ
 33.         81.         153.      13.77      4600.      3.024      50000.  1
 .0429       1152000.    1.25      2000.                                   2
 1-03        2.          0         0          4.134      1500.           3
    .00      4500.                                                        4
    .10      4500.                                                        5
    .20      4500.                                                        6
    .35      4500.                                                        7
    .50      4500.                                                        8
```

1.00	4500.					9
2.00	4500.					10
3.50	4500.					11
4.00	2800.					12
4.25	2600.					13
4.50	2350.					14
5.00	1900.					15
5.25	1650.					16
5.50	1400.					17
6.00	1000.					18
10.00	1000.					19
30.00	1000.					20
40.00	1000.					21
50.00	1000.					22
60.00	1000.					23
.6325	3670150.	1.264	31.08	2433.	.0567	24
.5079-03	.8497	.0478	.0194	.2453	1.	25
2.1356	3670150.	1.264	31.08	2433.	.0567	26
.5079-03	.8497	.1344	.0142	.3127	7.	27

PROB

APPENDIX C

Input and Output Data

1. Input Data
2. Output Data
3. Sample of Output Format

1. INPUT DATA

	Units	Program Symbol
Gun Constants		
Weight of Projectile	lb	WP
Length of Gun Tube	in.	XM
Empty Volume of Chamber	$in.^3$	VO
Cross-sectional Area of Bore	$in.^2$	AP
Shot-Start Pressure	psi	PE
Pidduck-Kent Constant	dimensionless	DEL
Resistive Pressures	psi	PR1,J
Travel of Projectile Corresponding to each of 20 Resistive Pressures	in.	XC1,J
Diameter of Bore	in.	D
Propellant Physical Constants		
Weights of Propellants	lb	C1,J
Weight of Igniter	lb	CI
Densities of Propellants	$lb/in.^3$	RHO1,J
Outside Diameter of Propellant Grains	in.	D1,J
Diameter of Propellant Perforations	in.	DP1,J
Length of Propellant Grains	in.	L1,J
Number of Perforations per Grain	dimensionless	NP1,J
Number of Propellants	dimensionless	N1
Propellant Thermodynamic Constants*		
Forces of Propellants	in.-lb/lb	F1,J
Force of Igniter	in.-lb/lb	FI

* See Reference (17) for these data.

	Units	Program Symbol
Ratios of Specific Heats of Propellants	dimensionless	GA1,J
Ratio of Specific Heats of Igniter	dimensionless	GAI
Covolumes of Propellants	$in.^3/lb$	COV1,J
Adiabatic Flame Temperatures of Propellants	^oK	TO1,J
Adiabatic Flame Temperature of Igniter	^oK	TOI
Burning Rate Coefficients	$\frac{in.}{sec} - \frac{1}{psi^{\alpha}}$	BET1,J
Burning Rate Exponents (α's)	dimensionless	ALP1,J
Burning Rate Velocity Coefficient	$\frac{in.}{sec\ in./sec}$	KV
Burning Rate Displacement Coefficient	$\frac{in.}{sec\text{-}in.}$	KX
Miscellaneous Constants		
Time Interval	sec	DT
Estimated Muzzle Velocity	ft /sec	EVP
Maximum Allowable Breech Pressure	psi	PPMAX

2. OUTPUT DATA

Identifying Data

The complete list of input data is printed out to permanently identify the computation.

	Units	Program Symbol
Trajectory Data		
Time	millisec	TM
Travel of Projectile	in.	XI
Travel of Projectile	ft	XF
Breech Pressure	psi	PBR
Space-mean Pressure	psi	PT
Base Pressure	psi	PB
Velocity of Projectile	ft/sec	V
Acceleration of Projectile	ft/sec^2	AF
Temperature of Propellant Gas	^oK	TEMP
Volume behind Projectile available for Propellant Gas	$in.^3$	VC
Resistive Pressure	psi	PR
Total Surface Area of Propellants	$in.^2$	ST
Mass-fractions of Propellants Burned	dimensionless	Y3,J
Mass Burning Rates of Propellants	lb/sec	DCZ1,J
Linear Burning Rates of Propellants	in./sec	R1,J
Surface Areas of Propellants	$in.^2$	S1,J

OUTPUT FORMAT

105 MM HOWITZER - RD 765

PROJ. WT.	BARREL	CHAMBER	BORE AREA	P-K	SS PRESS	MAX GUN PRESSURE
33.00000	81.00000	154.00000	13.77000	3.02400	4600.	50000.

M1 PROPELLANT

CHARGE	FORCE	GAMMA	COVOLUME	FLAME TEMP	DENSITY	
.04290	1152000.	1.2500		2000.		IGNITER
.63250	3670150.	1.2640	31.080	2433.	.056700	
2.13560	3670150.	1.2640	31.080	2433.	.056700	

BETA	ALPHA	O.D. GRAIN DIA.	PERF GR.	LENGTH	NO. PERF.
.0005079	.8497	.0478	.0194	.2453	1.
.0005079	.8497	.1344	.0142	.3127	7.

RESISTANCE

PROJ. TRAVEL	PRESSURE
.000	4500.
.100	4500.
.200	4500.
.350	4500.
.500	4500.
1.000	4500.
2.000	4500.
3.500	4500.
4.000	2800.
4.250	2600.
4.500	2350.
5.000	1900.
5.250	1650.
5.500	1400.
6.000	1000.
10.000	1000.
30.000	1000.
40.000	1000.
50.000	1000.
60.000	1000.

MISCELLANEOUS

DT	NO. PROP.	KV	KX	EST. MUZ. VEL.	DIAMETER
.00010	2.	.0000000	.0000000	1500.	4.1340

105 MM HOWITZER RD 765

* TM=.1000	XI=.000	PBR= 559.30	PT= 559.30	PB=559.30	V= .00	AF= .0000
TM=.1000	XI=.000	XF=.0000	TMP=2053.25	VC=104.147	PR=.0	ST=4018.93
TM=.1000	XI=.000	Y3=.0015	DC21= 9.601	R1=.102	S1=1661.83	
TM=.1000	XI=.000	Y4=.0006	DC22=13.618	R2=.102	S2=2357.10	
.2000	.000	651.34	651.34	651.34	.00	.0000
.2000	.000	.0000	2097.81	104.112	.0	4019.58
.2000	.000	.0032	10.945	.116	1661.54	
.2000	.000	.0013	15.533	.116	2358.04	
.3000	.000	756.33	756.33	756.33	.00	.0000
.3000	.000	.0000	2137.31	104.072	.0	4020.31
.3000	.000	.0051	12.444	.132	1661.20	
.3000	.000	.0022	17.671	.132	2359.10	
.4000	.000	875.66	875.66	875.66	.00	.0000
.4000	.000	.0000	2172.18	104.026	.0	4021.14
.4000	.000	.0073	14.112	.150	1660.82	
.4000	.000	.0031	20.055	.150	2360.31	
.5000	.000	1010.97	1010.97	1010.97	.00	.0000
.5000	.000	.0000	2202.89	103.975	.0	4022.07
.5000	.000	.0098	15.963	.170	1660.39	
.5000	.000	.0041	22.706	.170	2361.68	
.6000	.000	1164.02	1164.02	1164.02	.00	.0000
.6000	.000	.0000	2229.89	103.917	.0	4023.13
.6000	.000	.0126	18.015	.191	1659.91	
.6000	.000	.0053	25.648	.191	2363.22	
.7000	.000	1336.74	1336.74	1336.74	.00	.0000
.7000	.000	.0000	2253.61	103.851	.0	4024.32
.7000	.000	.0158	20.283	.216	1659.36	
.7000	.000	.0066	28.907	.216	2364.96	
.8000	.000	1531.26	1531.26	1531.26	.00	.0000
.8000	.000	.0000	2274.43	103.777	.0	4025.66
.8000	.000	.0193	22.785	.242	1658.74	
.8000	.000	.0081	32.513	.242	2366.91	
.9000	.000	1749.89	1749.89	1749.89	.00	.0000
.9000	.000	.0000	2292.69	103.695	.0	4027.15
.9000	.000	.0233	25.542	.272	1658.05	
.9000	.000	.0098	36.496	.272	2369.10	
1.0000	.000	1995.16	1995.16	1995.16	.00	.0000
1.0000	.000	.0000	2308.72	103.602	.0	4028.83
1.0000	.000	.0278	28.574	.304	1657.28	
1.0000	.000	.0117	40.889	.304	2371.55	
1.1000	.000	2269.85	2269.85	2269.85	.00	.0000
1.1000	.000	.0000	2322.79	103.499	.0	4030.70
1.1000	.000	.0328	31.903	.340	1656.42	
1.1000	.000	.0138	45.729	.340	2374.28	

*See list of Output Data for Program Symbols and Units.

105 MM HOWITZER - AD 765

1.2000	.000	2577.01	2577.01	2577.01	.00	.0000
1.2000	.000	.0000	2335.15	103.383	.0	4032.78
1.2000	.000	.0383	35.552	.379	1655.46	
1.2000	.000	.0162	51.055	.379	2377.32	
1.3000	.000	2919.97	2919.97	2919.97	.00	.0000
1.3000	.000	.0000	2346.02	103.255	.0	4035.09
1.3000	.000	.0445	39.548	.422	1654.38	
1.3000	.000	.0188	56.911	.422	2380.70	
1.4000	.000	3302.38	3302.38	3302.38	.00	.0000
1.4000	.000	.0000	2355.58	103.112	.0	4037.66
1.4000	.000	.0514	43.918	.469	1653.19	
1.4000	.000	.0217	63.344	.469	2384.46	
1.5000	.000	3728.28	3728.28	3728.28	.00	.0000
1.5000	.000	.0000	2364.00	102.953	.0	4040.50
1.5000	.000	.0590	48.690	.520	1651.87	
1.5000	.000	.0250	70.407	.520	2388.62	
1.6000	.000	4202.09	4202.09	4202.09	.00	.0000
1.6000	.000	.0000	2371.43	102.777	.0	4043.64
1.6000	.000	.0674	53.898	.576	1650.41	
1.6000	.000	.0286	78.156	.576	2393.23	
1.7000	.000	4728.68	4728.68	4728.68	.00	.0000
1.7000	.000	.0000	2377.98	102.582	.0	4047.11
1.7000	.000	.0767	59.574	.637	1648.79	
1.7000	.000	.0326	86.655	.637	2398.32	
1.8000	.000	5384.73	5312.49	5169.10	1.49	8990.2031
1.8000	.000	.0000	2383.69	102.382	4500.0	4050.93
1.8000	.000	.0870	65.753	.704	1647.00	
1.8000	.000	.0371	95.972	.704	2403.93	
1.9000	.004	6040.79	5959.75	5798.89	2.77	17452.175
1.9000	.004	.0003	2388.72	102.162	4500.0	4055.14
1.9000	.004	.0983	72.457	.777	1645.03	
1.9000	.004	.0420	106.156	.777	2410.11	
2.0000	.009	6765.89	6675.12	6494.96	4.94	26804.618
2.0000	.009	.0007	2393.04	101.946	4500.0	4059.76
2.0000	.009	.1108	79.730	.856	1642.85	
2.0000	.009	.0474	117.296	.856	2416.91	
2.1000	.016	7565.33	7463.83	7262.38	8.08	37115.875
2.1000	.016	.0014	2396.65	101.739	4500.0	4064.83
2.1000	.016	.1245	87.594	.942	1640.46	
2.1000	.016	.0534	129.452	.942	2424.37	
2.2000	.028	8444.01	8330.73	8105.88	12.30	48449.250
2.2000	.028	.0024	2399.56	101.556	4500.0	4070.38
2.2000	.028	.1395	96.069	1.035	1637.83	
2.2000	.028	.0600	142.686	1.035	2432.55	

105 MM HOWITZER RD 765

2.3000	.046	9406.19	9280.00	9029.53	17.70	60859.566
2.3000	.046	.0039	2401.74	101.410	4500.0	4076.44
2.3000	.046	.1560	105.169	1.134	1634.94	
2.3000	.046	.0672	157.052	1.134	2441.50	
2.4000	.071	10455.21	10314.94	10036.54	24.38	74389.969
2.4000	.071	.0059	2403.13	101.320	4500.0	4083.05
2.4000	.071	.1740	114.896	1.242	1631.78	
2.4000	.071	.0752	172.598	1.242	2451.28	
2.5000	.105	11593.13	11437.59	11128.89	32.46	89066.992
2.5000	.105	.0088	2403.70	101.304	4500.0	4090.24
2.5000	.105	.1936	125.241	1.357	1628.32	
2.5000	.105	.0840	189.356	1.357	2461.92	
2.6000	.150	12820.27	12648.27	12306.89	42.05	104894.83
2.6000	.150	.0125	2403.38	101.383	4500.0	4098.04
2.6000	.150	.2150	136.177	1.478	1624.55	
2.6000	.150	.0936	207.338	1.478	2473.48	
2.7000	.207	14134.69	13945.06	13568.68	53.26	121848.41
2.7000	.207	.0172	2402.12	101.579	4500.0	4106.47
2.7000	.207	.2382	147.660	1.607	1620.45	
2.7000	.207	.1041	226.532	1.607	2486.01	
2.8000	.278	15531.68	15323.30	14909.72	66.19	139866.91
2.8000	.278	.0232	2399.83	101.916	4500.0	4115.55
2.8000	.278	.2633	159.622	1.742	1616.01	
2.8000	.278	.1155	246.895	1.742	2499.55	
2.9000	.366	17003.23	16775.11	16322.35	80.93	158847.23
2.9000	.366	.0305	2396.46	102.421	4500.0	4125.31
2.9000	.366	.2904	171.973	1.882	1611.19	
2.9000	.366	.1280	268.348	1.882	2514.12	
3.0000	.473	18537.66	18288.95	17795.33	97.58	178638.52
3.0000	.473	.0394	2391.94	103.123	4500.0	4135.75
3.0000	.473	.3196	184.593	2.027	1606.01	
3.0000	.473	.1415	290.767	2.027	2529.75	
3.1000	.601	20119.30	19849.37	19313.63	116.20	199038.64
3.1000	.601	.0501	2386.20	104.050	4500.0	4146.87
3.1000	.601	.3508	197.338	2.175	1600.43	
3.1000	.601	.1561	313.984	2.175	2546.44	
3.2000	.753	21728.45	21436.93	20858.35	136.82	219793.76
3.2000	.753	.0628	2379.19	105.235	4500.0	4158.66
3.2000	.753	.3840	210.040	2.323	1594.47	
3.2000	.753	.1719	337.780	2.323	2564.18	
3.3000	.931	23341.69	23028.53	22406.98	159.46	240601.50
3.3000	.931	.0776	2370.87	106.710	4500.0	4171.09
3.3000	.931	.4193	222.506	2.471	1588.12	
3.3000	.931	.1888	361.890	2.471	2582.96	

105 MM HOWITZER - RD 765

3.4000	1.137	24932.43	24597.93	23934.03	184.10	261119.19
3.4000	1.137	.0947	2361.21	108.510	4500.0	4184.12
3.4000	1.137	.4566	234.532	2.616	1581.39	
3.4000	1.137	.2068	386.006	2.616	2602.74	
3.5000	1.373	26471.99	26116.83	25411.94	210.69	280976.61
3.5000	1.373	.1144	2350.23	110.667	4500.0	4197.72
3.5000	1.373	.4958	245.905	2.755	1574.29	
3.5000	1.373	.2260	409.784	2.755	2623.44	
3.6000	1.643	27930.86	27556.13	26812.39	239.13	299793.28
3.6000	1.643	.1369	2337.93	113.217	4500.0	4211.82
3.6000	1.643	.5367	256.417	2.886	1566.83	
3.6000	1.643	.2464	432.862	2.886	2644.99	
3.7000	1.948	29280.32	28887.48	28107.81	269.31	317198.79
3.7000	1.948	.1625	2324.36	116.192	4500.0	4226.35
3.7000	1.948	.5792	265.874	3.008	1559.05	
3.7000	1.948	.2678	454.872	3.008	2667.31	
3.8000	2.290	30494.10	30084.98	29272.98	301.06	332854.33
3.8000	2.290	.1908	2309.60	119.625	4500.0	4241.23
3.8000	2.290	.6232	274.108	3.117	1550.97	
3.8000	2.290	.2902	475.458	3.117	2690.26	
3.9000	2.671	31549.96	31126.67	30286.56	334.20	346472.95
3.9000	2.671	.2226	2293.75	123.545	4500.0	4256.38
3.9000	2.671	.6683	280.985	3.212	1542.63	
3.9000	2.671	.3135	494.300	3.212	2713.75	
4.0000	3.092	32430.96	31995.85	31132.28	368.50	357836.18
4.0000	3.092	.2577	2276.91	127.981	4500.0	4271.70
4.0000	3.092	.7144	286.417	3.293	1534.07	
4.0000	3.092	.3377	511.126	3.293	2737.63	
4.1000	3.555	33126.32	32681.88	31799.80	403.76	366805.04
4.1000	3.555	.2963	2259.23	132.956	4353.8	4287.10
4.1000	3.555	.7612	290.358	3.357	1525.33	
4.1000	3.555	.3626	525.726	3.357	2761.77	
4.2000	4.061	33634.57	33183.32	32287.70	440.69	385840.09
4.2000	4.061	.3384	2241.04	138.493	2710.8	4302.49
4.2000	4.061	.8085	292.834	3.406	1516.45	
4.2000	4.061	.3882	538.002	3.406	2786.05	
4.3000	4.614	33945.68	33490.25	32586.35	479.72	403930.04
4.3000	4.614	.3845	2221.95	144.626	2241.9	4317.80
4.3000	4.614	.8561	293.805	3.437	1507.47	
4.3000	4.614	.4142	547.733	3.437	2810.33	
4.4000	5.213	34063.00	33605.99	32698.97	519.69	412771.20
4.4000	5.213	.4344	2202.25	151.390	1688.0	4332.93
4.4000	5.213	.9036	295.326	3.452	1498.44	
4.4000	5.213	.4406	554.862	3.452	2834.49	

105 MM HOWITZER RD 765

4.5000	5.861	33997.55	33541.42	32636.14	560.46	420082.51
4.5000	5.861	.4884	2182.08	158.810	1097.9	4347.82
4.5000	5.861	.9509	291.497	3.452	1489.41	
4.5000	5.861	.4673	559.430	3.452	2858.42	
4.6000	6.558	33762.85	33309.87	32410.84	601.73	423888.90
4.6000	6.558	.5465	2161.52	166.904	658.5	4362.40
4.6000	6.558	.9977	288.442	3.436	1480.40	
4.6000	6.558	.4941	561.529	3.436	2882.00	
4.7000	7.305	32683.80	32245.30	31375.00	642.69	414921.60
4.7000	7.305	.6087	2135.99	176.078	374.8	2904.82
4.7000	7.305	1.0000	.000	.000	.00	
4.7000	7.305	.5208	556.704	3.380	2904.82	
4.8000	8.100	31546.35	31123.11	30283.10	682.55	402787.92
4.8000	8.100	.6750	2110.52	185.947	290.7	2926.94
4.8000	8.100	1.0000	.000	.000	.00	
4.8000	8.100	.5469	544.755	3.283	2926.94	
4.9000	8.942	30382.32	29974.70	29165.68	720.95	387359.05
4.9000	8.942	.7452	2085.45	196.490	446.6	2948.17
4.9000	8.942	1.0000	.000	.000	.00	
4.9000	8.942	.5724	531.861	3.182	2948.17	
5.0000	9.829	29211.63	28819.72	28041.87	757.55	368342.90
5.0000	9.829	.8191	2060.93	207.686	863.7	2968.51
5.0000	9.829	1.0000	.000	.000	.00	
5.0000	9.829	.5973	518.326	3.080	2968.51	
5.1000	10.759	28052.88	27676.52	26929.53	792.17	348393.83
5.1000	10.759	.8966	2037.15	219.504	1000.0	2987.98
5.1000	10.759	1.0000	.000	.000	.00	
5.1000	10.759	.6215	504.441	2.977	2987.98	
5.2000	11.729	26920.30	26559.13	25842.29	825.32	333785.59
5.2000	11.729	.9774	2014.27	231.916	1000.0	3006.61
5.2000	11.729	1.0000	.000	.000	.00	
5.2000	11.729	.6451	490.446	2.877	3006.61	
5.3000	12.739	25820.59	25474.17	24786.62	857.08	319601.38
5.3000	12.739	1.0616	1992.15	244.894	1000.0	3024.42
5.3000	12.739	1.0000	.000	.000	.00	
5.3000	12.739	.6679	476.475	2.779	3024.42	
5.4000	13.785	24760.24	24428.04	23768.73	887.50	305924.79
5.4000	13.785	1.1488	1970.86	258.417	1000.0	3041.46
5.4000	13.785	1.0000	.000	.000	.00	
5.4000	13.785	.6901	462.663	2.683	3041.46	
5.5000	14.868	23743.17	23424.62	22792.39	916.62	292806.55
5.5000	14.868	1.2390	1950.39	272.461	1000.0	3057.75
5.5000	14.868	1.0000	.000	.000	.00	
5.5000	14.868	.7117	449.108	2.590	3057.75	

105 MM HOWITZER RD 765

5.6000	15.985	22771.60	22466.08	21859.72	944.52	280275.03
5.6000	15.985	1.3320	1930.73	287.005	1000.0	3073.33
5.6000	15.985	1.0000	.000	.000	.00	
5.6000	15.985	.7326	435.883	2.501	3073.33	
5.7000	17.134	21846.41	21553.31	20971.58	971.23	268341.81
5.7000	17.134	1.4278	1911.87	302.027	1000.0	3088.25
5.7000	17.134	1.0000	.000	.000	.00	
5.7000	17.134	.7529	423.041	2.416	3088.25	
5.8000	18.315	20967.52	20686.21	20127.89	996.83	257005.85
5.8000	18.315	1.5262	1893.78	317.509	1000.0	3102.53
5.8000	18.315	1.0000	.000	.000	.00	
5.8000	18.315	.7725	410.617	2.338	3102.53	
5.9000	19.526	20134.15	19864.02	19327.89	1021.37	246256.84
5.9000	19.526	1.6271	1876.45	333.431	1000.0	3116.21
5.9000	19.526	1.0000	.000	.000	.00	
5.9000	19.526	.7916	398.631	2.256	3116.21	
6.0000	20.766	19344.97	19085.43	18570.31	1044.89	236077.89
6.0000	20.766	1.7305	1859.83	349.774	1000.0	3129.33
6.0000	20.766	1.0000	.000	.000	.00	
6.0000	20.766	.8102	387.097	2.182	3129.33	
6.1000	22.033	18598.33	18348.81	17853.57	1067.47	226447.66
6.1000	22.033	1.8361	1843.90	366.521	1000.0	3141.92
6.1000	22.033	1.0000	.000	.000	.00	
6.1000	22.033	.8282	376.015	2.111	3141.92	
6.2000	23.327	17892.36	17652.31	17175.87	1089.14	217341.96
6.2000	23.327	1.9439	1828.63	383.657	1000.0	3154.01
6.2000	23.327	1.0000	.000	.000	.00	
6.2000	23.327	.8456	365.384	2.043	3154.01	
6.3000	24.646	17225.06	16993.96	16535.29	1109.95	208735.00
6.3000	24.646	2.0539	1813.99	401.165	1000.0	3165.63
6.3000	24.646	1.0000	.000	.000	.00	
6.3000	24.646	.8626	355.196	1.979	3165.63	
6.4000	25.990	16594.37	16371.73	15929.86	1129.96	200600.28
6.4000	25.990	2.1659	1799.94	419.030	1000.0	3176.79
6.4000	25.990	1.0000	.000	.000	.00	
6.4000	25.990	.8791	345.439	1.918	3176.79	
6.5000	27.358	15998.23	15783.60	15357.60	1149.21	192911.28
6.5000	27.358	2.2798	1786.45	437.239	1000.0	3187.54
6.5000	27.358	1.0000	.000	.000	.00	
6.5000	27.358	.8952	336.099	1.860	3187.54	
6.6000	28.748	15434.64	15227.56	14816.57	1167.73	185641.93
6.6000	28.748	2.3957	1773.51	455.779	1000.0	3197.89
6.6000	28.748	1.0000	.000	.000	.00	
6.6000	28.748	.9108	327.163	1.804	3197.89	

105 MM HOWITZER RD 765

6.7000	30.160	14901.62	14701.69	14304.89	1185.57	178766.98
6.7000	30.160	2.5133	1761.07	474.637	1000.0	3207.87
6.7000	30.160	1.0000	.000	.000	.00	
6.7000	30.160	.9260	318.613	1.752	3207.87	
6.8000	31.593	14397.30	14204.14	13820.77	1202.76	172262.16
6.8000	31.593	2.6327	1749.12	493.801	1000.0	3217.50
6.8000	31.593	1.0000	.000	.000	.00	
6.8000	31.593	.9408	310.434	1.702	3217.50	
6.9000	33.046	13919.88	13733.13	13362.47	1219.34	166104.36
6.9000	33.046	2.7539	1737.63	513.260	1000.0	3226.79
6.9000	33.046	1.0000	.000	.000	.00	
6.9000	33.046	.9552	302.608	1.654	3226.79	
7.0000	34.519	13467.67	13286.98	12928.37	1235.34	160271.72
7.0000	34.519	2.8766	1726.57	533.003	1000.0	3235.76
7.0000	34.519	1.0000	.000	.000	.00	
7.0000	34.519	.9693	295.119	1.609	3235.76	
7.1000	36.011	13039.07	12864.14	12516.93	1250.79	154743.60
7.1000	36.011	3.0009	1715.92	553.021	1000.0	3244.44
7.1000	36.011	1.0000	.000	.000	.00	
7.1000	36.011	.9830	287.950	1.565	3244.44	
7.2000	37.521	12632.58	12463.10	12126.72	1265.71	149500.65
7.2000	37.521	3.1267	1705.66	573.304	1000.0	3252.83
7.2000	37.521	1.0000	.000	.000	.00	
7.2000	37.521	.9964	281.086	1.524	3252.83	
7.3000	39.048	12113.37	11950.85	11628.29	1280.08	142803.69
7.3000	39.048	3.2540	1690.38	594.117	1000.0	.00
7.3000	39.048	1.0000	.000	.000	.00	
7.3000	39.048	1.0000	.000	.000	.00	
7.4000	40.592	11581.18	11425.80	11117.42	1293.77	135939.51
7.4000	40.592	3.3827	1673.65	615.268	1000.0	.00
7.4000	40.592	1.0000	.000	.000	.00	
7.4000	40.592	1.0000	.000	.000	.00	
7.5000	42.153	11084.23	10935.52	10640.37	1306.80	129529.70
7.5000	42.153	3.5127	1657.49	636.645	1000.0	.00
7.5000	42.153	1.0000	.000	.000	.00	
7.5000	42.153	1.0000	.000	.000	.00	
7.6000	43.728	10619.56	10477.09	10194.31	1319.24	123536.40
7.6000	43.728	3.6440	1641.86	658.238	1000.0	.00
7.6000	43.728	1.0000	.000	.000	.00	
7.6000	43.728	1.0000	.000	.000	.00	
7.7000	45.319	10184.55	10047.91	9776.72	1331.10	117925.56
7.7000	45.319	3.7766	1626.75	680.036	1000.0	.00
7.7000	45.319	1.0000	.000	.000	.00	
7.7000	45.319	1.0000	.000	.000	.00	

105 MM HOWITZER - RD 765

7.8000	46.923	9776.80	9645.63	9385.29	1342.44	112666.32
7.8000	46.923	3.9102	1612.13	702.030	1000.0	.00
7.8000	46.923	1.0000	.000	.000	.00	
7.8000	46.923	1.0000	.000	.000	.00	
7.9000	48.540	9394.13	9268.10	9017.95	1353.28	107730.66
7.9000	48.540	4.0450	1597.98	724.211	1000.0	.00
7.9000	48.540	1.0000	.000	.000	.00	
7.9000	48.540	1.0000	.000	.000	.00	
8.0000	50.170	9034.59	8913.38	8672.80	1363.65	103093.19
8.0000	50.170	4.1809	1584.27	746.572	1000.0	.00
8.0000	50.170	1.0000	.000	.000	.00	
8.0000	50.170	1.0000	.000	.000	.00	
8.1000	51.813	8696.37	8579.69	8348.13	1373.58	98730.794
8.1000	51.813	4.3177	1570.98	769.104	1000.0	.00
8.1000	51.813	1.0000	.000	.000	.00	
8.1000	51.813	1.0000	.000	.000	.00	
8.2000	53.467	8377.85	8265.45	8042.36	1383.09	94622.489
8.2000	53.467	4.4556	1558.10	791.800	1000.0	.00
8.2000	53.467	1.0000	.000	.000	.00	
8.2000	53.467	1.0000	.000	.000	.00	
8.3000	55.132	8077.55	7969.18	7754.09	1392.22	90749.161
8.3000	55.132	4.5943	1545.61	814.654	1000.0	.00
8.3000	55.132	1.0000	.000	.000	.00	
8.3000	55.132	1.0000	.000	.000	.00	
8.4000	56.808	7794.12	7689.55	7482.01	1400.98	87093.400
8.4000	56.808	4.7340	1533.49	837.658	1000.0	.00
8.4000	56.808	1.0000	.000	.000	.00	
8.4000	56.808	1.0000	.000	.000	.00	
8.5000	58.494	7526.32	7425.34	7224.93	1409.39	83639.325
8.5000	58.494	4.8745	1521.73	860.807	1000.0	.00
8.5000	58.494	1.0000	.000	.000	.00	
8.5000	58.494	1.0000	.000	.000	.00	
8.6000	60.190	7273.04	7175.46	6981.79	1417.47	80372.437
8.6000	60.190	5.0159	1510.30	884.096	1000.0	.00
8.6000	60.190	1.0000	.000	.000	.00	
8.6000	60.190	1.0000	.000	.000	.00	
8.7000	61.896	7033.24	6938.88	6751.60	1425.23	77279.479
8.7000	61.896	5.1580	1499.19	907.517	1000.0	.00
8.7000	61.896	1.0000	.000	.000	.00	
8.7000	61.896	1.0000	.000	.000	.00	
8.8000	63.611	6805.98	6714.67	6533.44	1432.71	74348.324
8.8000	63.611	5.3009	1488.40	931.067	1000.0	.00
8.8000	63.611	1.0000	.000	.000	.00	
8.8000	63.611	1.0000	.000	.000	.00	

105 MM HOWITZER RD 765

8.9000	65.334	6590.41	6501.99	6326.50	1439.90	71567.857
8.9000	65.334	5.4445	1477.90	954.741	1000.0	.00
8.9000	65.334	1.0000	.000	.000	.00	
8.9000	65.334	1.0000	.000	.000	.00	
9.0000	67.066	6385.73	6300.06	6130.02	1446.86	68927.685
9.0000	67.066	5.5889	1467.69	978.533	1000.0	.00
9.0000	67.066	1.0000	.000	.000	.00	
9.0000	67.066	1.0000	.000	.000	.00	
9.1000	68.807	6191.22	6108.16	5943.38	1453.50	66419.046
9.1000	68.807	5.7339	1457.75	1002.440	1000.0	.00
9.1000	68.807	1.0000	.000	.000	.00	
9.1000	68.807	1.0000	.000	.000	.00	
9.2000	70.555	6006.21	5925.63	5765.69	1459.94	64032.734
9.2000	70.555	5.8796	1448.07	1026.457	1000.0	.00
9.2000	70.555	1.0000	.000	.000	.00	
9.2000	70.555	1.0000	.000	.000	.00	
9.3000	72.310	5830.08	5751.86	5596.62	1466.14	61761.028
9.3000	72.310	6.0259	1438.64	1050.581	1000.0	.00
9.3000	72.310	1.0000	.000	.000	.00	
9.3000	72.310	1.0000	.000	.000	.00	
9.4000	74.073	5662.27	5586.31	5435.53	1472.13	59596.629
9.4000	74.073	6.1728	1429.45	1074.807	1000.0	.00
9.4000	74.073	1.0000	.000	.000	.00	
9.4000	74.073	1.0000	.000	.000	.00	
9.5000	75.843	5502.27	5428.44	5281.93	1477.91	57532.803
9.5000	75.843	6.3203	1420.49	1099.132	1000.0	.00
9.5000	75.843	1.0000	.000	.000	.00	
9.5000	75.843	1.0000	.000	.000	.00	
9.6000	77.620	5349.57	5277.80	5135.35	1483.49	55563.332
9.6000	77.620	6.4683	1411.76	1123.553	1000.0	.00
9.6000	77.620	1.0000	.000	.000	.00	
9.6000	77.620	1.0000	.000	.000	.00	
9.7000	79.404	5203.75	5133.93	4995.37	1488.89	53682.469
9.7000	79.404	6.6170	1403.24	1148.066	1000.0	.00
9.7000	79.404	1.0000	.000	.000	.00	
9.7000	79.404	1.0000	.000	.000	.00	
9.8000	81.193	5064.38	4996.43	4861.58	1494.10	51884.892
9.8000	81.193	6.7661	1394.92	1172.668	1000.0	.00
9.8000	81.193	1.0000	.000	.000	.00	
9.8000	81.193	1.0000	.000	.000	.00	

MUZZLE VEL.	MAX. PRESSURE	X AT PMAX	T AT PMAX	MUZ PRESSURE
1493.5	34063.	5.213	4.400	4876.0

APPENDIX D

Comparison of Experimental and Predicted Performance for Typical 105mm Howitzer Firing

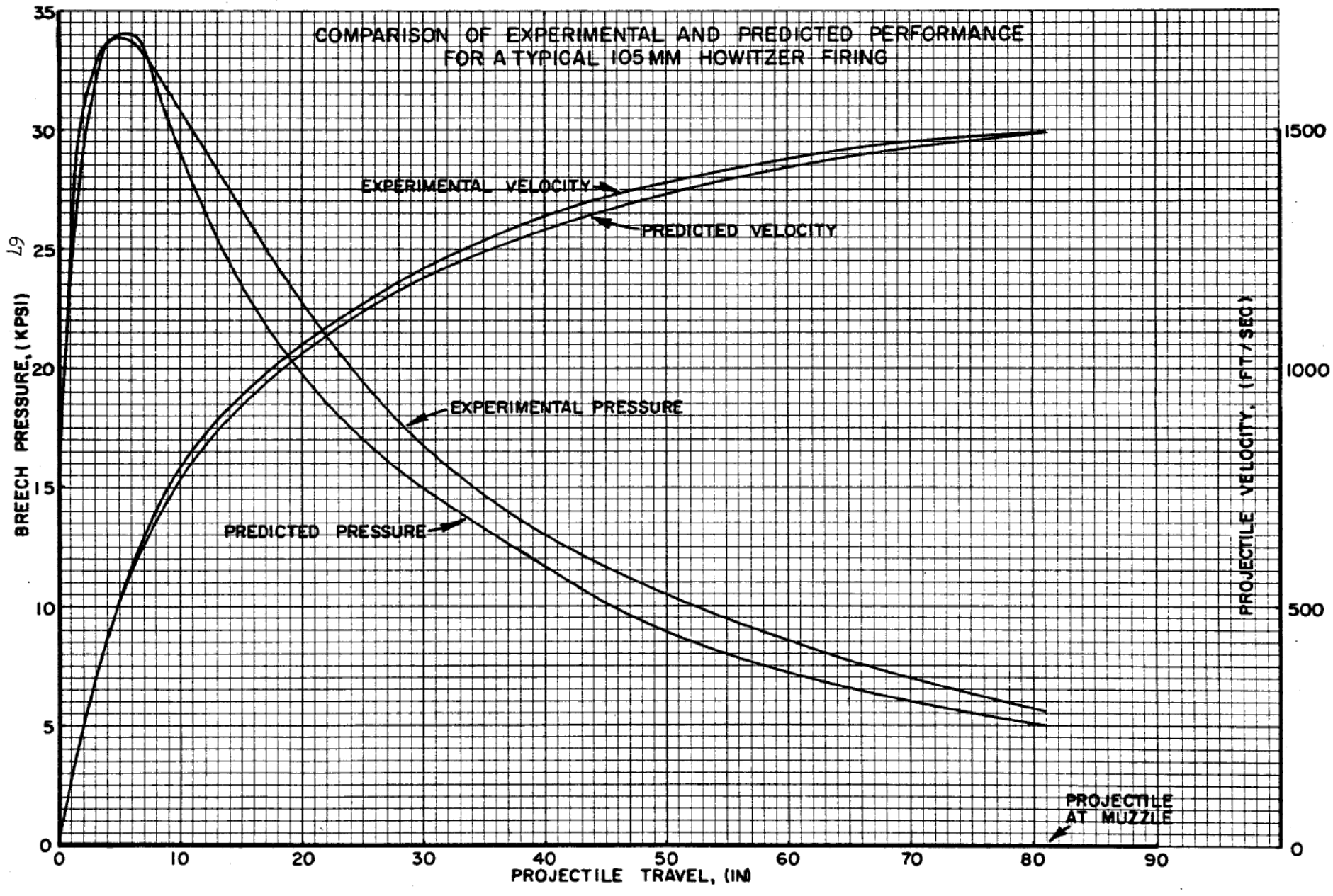
COMPARISON OF EXPERIMENTAL AND PREDICTED PERFORMANCE
FOR A TYPICAL 105 MM HOWITZER FIRING
EXPERIMENTAL VELOCITY
PREDICTED VELOCITY
EXPERIMENTAL PRESSURE
PREDICTED PRESSURE
PROJECTILE AT MUZZLE
BREECH PRESSURE, (KPSI)
PROJECTILE VELOCITY, (FT/SEC)
PROJECTILE TRAVEL, (IN)
0
5
10
15
20
25
30
35
0
500
1000
1500
0
10
20
30
40
50
60
70
80
90

ERRATA-BRLR 1183

pg 8 m_i specific mass of i th propellant, lb-mol/lb

pg 9 R Universal Gas Constant, in-lb/lb-mol-°K

T_s initial temperature of gun, °K

pg 14 $\bar{c}_{p_i} - \bar{c}_{v_i} = m_i R$

pg 15 dx (in Eq(14))

pg 16 and pg 23

$$E_h = \frac{12x0.38c^{1.5}\left(x_m + \frac{V_o}{A}\right)\left(\frac{\sum_{i=1}^{n} C_i \, To_i}{\sum_{i=1}^{n} C_i} - T_s\right) v^2}{\left[1 + \frac{0.6c^{2.175}}{\left(\sum_{i=1}^{n} C_i\right)^{0.8375}}\right] v_m^2}$$

pg 19 and pg 24

$$p_o = \frac{p_b}{(1-a_o)^{n'+1}}$$

pg 46 B16 IF (Y1>0)GOTO(B17)%Y1=0% IF(Y3 etc

J. M. Frankle